# *E. coli* glycogen branching enzyme restores synthesis of starch-like polyglucans in an *Arabidopsis* mutant devoid of endogenous starch branching enzymes

**Running Title:** Synthesis of starch-like polyglucans by *E. coli* BE

Laura Boyer [1], Xavier Roussel [1], Adeline Courseaux [1], Ofilia Mvundza Ndjindji [2,3], Christine Lancelon-Pin [2,3], Jean-Luc Putaux [2,3], Ian Tetlow [4], Michael Emes [4], Bruno Pontoire [5], Christophe D'Hulst [1] and Fabrice Wattebled [1,*]

[1] Unité de Glycobiologie Structurale et Fonctionnelle, UMR8576 CNRS – Université de Lille, F-59655 Villeneuve d'Ascq cedex, France

[2] Université Grenoble Alpes, Centre de Recherches sur les Macromolécules Végétales (CERMAV), F-38000 Grenoble, France

[3] CNRS, CERMAV, F-38000 Grenoble, France

[4] Department of Molecular and Cellular Biology, Science Complex, University of Guelph, Guelph, Ontario N1G 2W1, Canada

[5] UR1268 BIA, INRA, F-44300 Nantes, France

[*] Corresponding author: fabrice.wattebled@univ-lille1.fr

Total word count: 7740

## ABSTRACT

Starch synthesis requires several enzymatic activities including branching enzymes (BEs) responsible for the formation of α(1→6) linkages. Distribution and number of these linkages are further controlled by debranching enzymes (DBEs) that cleave some of them, rendering the polyglucan water-insoluble and semi-crystalline. Although the activity of BEs and DBEs is mandatory to sustain normal starch synthesis, the relative importance of each in the establishment of the plant storage polyglucan (i.e. water-insolubility, crystallinity, presence of amylose) is still debated. Here, we have substituted the activity of BEs in *Arabidopsis* with that of the *Escherichia coli* glycogen branching enzyme (GlgB). The latter is the BE counterpart in the metabolism of glycogen, a highly branched water-soluble and amorphous storage polyglucan. GlgB was expressed in the *be2 be3* double mutant of *Arabidopsis* that is devoid of BE activity and consequently free of starch. The synthesis of a water-insoluble, partly crystalline, amylose-containing starch-like polyglucan was restored in GlgB-expressing plants, suggesting that BEs only have a limited impact on establishing essential characteristics of starch. Moreover, the balance between branching and debranching is crucial for the synthesis of starch, as an excess of branching activity results in the formation of highly branched, water-soluble, poorly crystalline polyglucan.



## KEYWORDS

Starch, glycogen, α-glucan, polyglucan, branching enzyme, GlgB, *Arabidopsis thaliana*, *Escherichia coli*, debranching enzyme.

## INTRODUCTION

Amylopectin is one of the two homopolymers of glucose that constitute native starch in plants and algae. It is chemically identical to the glycogen found in bacteria, fungi and animals and is composed of glucosyl residues linked by α(1→4) O-glycosidic bonds and branched in α(1→6) linkages. However, the degree of branching of amylopectin does not exceed 5-6%, while it usually reaches 8 to 10% in glycogen (Buleon *et al.*, 1998; Roach *et al.*, 2012). Moreover, the distribution of α(1→6) linkages is different in both polyglucans. In glycogen, branch points are regularly distributed in the macromolecule, leading to the formation of a spherical homogenous structure with limited size (Melendez-Hevia *et al.*, 1993). On the other hand, amylopectin exhibits a heterogeneous molecular organization in which short linear segments are clustered and branch points form amorphous lamellae. Several models of cluster pattern have been proposed (Bertoft, 2013). Hizukuri's model suggests that clusters follow one another linearly. The clusters are linked together by longer glucans that expand from the preceding structure to the following (Hizukuri, 1986). More recently, Bertoft has proposed an alternative model in which clusters are linked side by side to a long, linear, glucan backbone (Bertoft, 2004). In Bertoft's model, the formation of a new cluster does not depend on the synthesis of a previous one. Regardless of which amylopectin model is considered, these differences between amylopectin and glycogen lead to different properties for both polymers. Amylopectin is water-insoluble and partly crystalline whereas glycogen is water-soluble and amorphous.

The biosynthesis of these polysaccharides involves the same set of enzymatic activities:

i. Polymerizing enzymes (i.e. starch- or glycogen-synthases) that transfer the glucose moiety of a nucleotide-sugar (being ADP-glucose or UDP-glucose) to the non-reducing end of an α-glucan by creating α(1→4) linkages (Fujita *et al.*, 2012).

ii. Branching enzymes (1,4-α-glucan:1,4-α-glucan 6-glucosyltransferase; EC 2.4.1.18) that introduce the α(1→6) branch points by rearranging linear glucans. These enzymes cleave an α(1→4) linkage and then transfer the released glucan in α(1→6) position by an intermolecular or intramolecular mechanism (Tetlow, 2012).

However, in the case of amylopectin, an additional activity is required to allow the formation of the specific structure of this macromolecule: an isoamylase-type debranching enzyme removes some of the α(1→6) linkages created by branching enzymes. This step appears mandatory since mutants lacking isoamylases exhibit a severe reduction in starch content and accumulate large amounts of a highly branched water-soluble and amorphous polyglucan called phytoglycogen (Mouille *et al.*, 1996; Myers *et al.*, 2000; Ball *et al.*, 2003; Wattebled *et al.*, 2005). Compared to wild-type starch, phytoglycogen displays significant modifications of chain length distribution characterized by enrichment in very short chains (DP 3-5). The crystallization of the polysaccharide clearly depends on the distribution of α(1→6) linkages, but also on chain length distribution (Pfister *et al.*, 2014). Starch synthases (by elongating glucans) and isoamylases (by removing some branch points) are key enzymes that control both parameters that are crucial to define the final structure and properties of starch. Modification of plant BE activity level can affect the physicochemical characteristics of starch as well. For instance, the reduction of branching enzyme activity in potato by the antisense inhibition of both SBE A and SBE B induces the

synthesis of very-high-amylose starch in potato tubers (Schwall *et al.*, 2000). In rice and maize, modification of BE activity (by mutation or over-expression) alters the structure and properties of the endosperm starch (Satoh *et al.*, 2003; Tanaka *et al.*, 2004; Yao *et al.*, 2004). Although it is obvious that BEs are mandatory for the synthesis of starch since these enzymes are the only one that create the α(1→6) linkages, their actual contribution for the determination of starch characteristics (i.e. water-insolubility, semi-crystallinity, presence of amylose, amylopectin $DP_{max}$ at 12-13) has not been precisely evaluated so far.

Branching enzymes (BEs) are classified into two groups depending on their amino-acid sequences: group I or B-family and group II or A-family (Burton *et al.*, 1995). The *in vitro* determination of catalytic parameters showed that BEI is more active on amylose than amylopectin, in contrast to the members of the BEII group (Guan *et al.*, 1993; Guan *et al.*, 1994). Moreover, BEI transfers longer glucans compared to BEII (Guan *et al.*, 1997). GlgB that generates α(1→6) linkages during glycogen synthesis has catalytic properties obviously distinct to that of maize BEII and BEI (Guan *et al.*, 1997).

In this work, our objective was to test whether the phylogenetic and family origin of BEs was crucial for the production of water-insoluble semi-crystalline polysaccharides. The expression of maize BEI or BEII or both BEI and BEII in a *glgB*- mutant of *E. coli* results in the synthesis of glycogen-like but not starch-like polysaccharides (Guan *et al.*, 1995). Similar results were obtained after the expression of maize BEIIa and/or BEIIb in a branching enzyme mutant of yeast (Seo *et al.*, 2002). Alternatively, *E. coli* glycogen branching enzyme (GlgB) was already expressed in different plants such as potato (Kortstee *et al.*, 1996; Huang *et al.*, 2013) and rice (Kim *et al.*, 2005) leading to modification of the structure of the synthesized polyglucans (increased branching degree

and altered chain length distribution of amylopectin). However in both cases, the endogenous BEs were still active, thus preventing from the determination of the specific contribution of GlgB for the synthesis of starch.

Arabidopsis contains only two BEs involved in transitory starch synthesis and both of them belong to the BEII group (Fisher *et al.*, 1996). Arabidopsis *be2 be3* double mutants are unable to create branch points during polysaccharide synthesis and are therefore starchless (Dumez *et al.*, 2006). We used these plants, devoid of endogenous BEs, to express the *E. coli* GlgB glycogen branching enzyme to evaluate whether enzyme metabolic origin (i.e. glycogen versus starch) can sustain the synthesis of starch-like polyglucan, more precisely, a polyglucan that is water-insoluble, partly crystalline, contain both amylopectin and amylose and in which amylopectin $DP_{max}$ is 12-13. GlgB is involved in the synthesis of glycogen and belongs to the BEI family (Sawada *et al.*, 2014). The analysis of polyglucan accumulation in *Arabidopsis* plants expressing GlgB revealed that the balance between branching and debranching activities, assuming that elongating activity is not-limiting, establishes the structure of the polysaccharide produced, regardless of the origin of the branching enzyme.

## MATERIALS AND METHODS

*Cloning of the glycogen branching enzyme (GlgB) of* Escherichia coli

The chloroplast transit peptide of *Arabidopsis thaliana* Branching Enzyme 2 (At5g03650) was identified with the use of ChloroP 1.1 (http://www.cbs.dtu.dk/services/ChloroP/). The corresponding nucleotide sequence was

136 reconstituted by PCR using two long and partially complementary primers, TPbe2-1 and
137 TPbe2-2 (primer sequences and method of amplification are depicted in details in Figure
138 S1). A fragment corresponding to the first 30 nucleotides of the 5' end of *glgB* was then
139 added downstream of the sequence encoding the transit peptide (Figure S1). In parallel, the
140 coding sequence of *glgB* was amplified by PCR from genomic DNA of *E. coli* TOP10
141 using primers glgB-For and glgB-Rev (Figure S1). The final sequence was obtained after
142 20 cycles of polymerase extension of both overlapping sequences. This chimeric cDNA
143 was subsequently amplified by PCR with primers TPbe2 for-CACC and glgB rev (Figure
144 S1) and cloned into pENTR™/D-TOPO prior to be transferred by homologous
145 recombination into pMDC32 using the gateway® technology (Life Technologies). The
146 sequence was checked by full-sequencing before further uses. All PCR reactions were
147 performed using a high-fidelity DNA polymerase (Kapa Hifi from KAPABIOSYSTEM®).
148
149 *Plant transformation and selection*
150 The *be2 be3* double mutant of *A. thaliana* (WS ecotype) (Dumez *et al.*, 2006) was
151 transformed by the floral dip method using *A. tumefaciens* strain GV3101 (Clough *et al.*,
152 1998; Jyothishwaran *et al.*, 2007) according to (Facon *et al.*, 2013). Transformed plants
153 were selected for their resistance to hygromycin B. T1 seeds were sterilized according to
154 (Harrison *et al.*, 2006) and sown on petri dishes containing 1% (w/v) Murashige and Skoog
155 medium, 1% (w/v) agar and 20 $\mu g.mL^{-1}$ of hygromycin B (Sigma-Aldrich). Plates were
156 incubated for 2-3 weeks at 22°C, 75% humidity and a specific photoperiod according to
157 (Harrison *et al.*, 2006). 98 hygromycin-resistant individuals were transferred to soil and
158 cultivated in a greenhouse under a 16-h light / 8-h dark photoperiod. The presence of the

159 transgene was confirmed by PCR amplification of the *glgB* sequence (glgB-For and glgB-
160 Rev primers) in 22 plants displaying a leaf iodine-staining phenotype (see below) different
161 to that of the *be2 be3* mother plant. A representative panel of eleven plants with different
162 leaf iodine-staining phenotypes was selected and T2 seeds were collected. T2 plants were
163 selected on solid MS medium as described above and 5 homozygous lines were identified by
164 segregation analysis of the hygromycin-resistance trait.
165
166 *Leaf iodine staining*
167 Approximately 3-week-old leaves were harvested at the end of the day and
168 immediately immersed in 70% hot ethanol. Samples were incubated under shaking at 70°C
169 and ethanol was replaced several times until complete loss of pigments, prior to be rinsed
170 with water and stained by a KI 1% (w/v) - $I_2$ 0.1% (w/v) solution.
171
172 *Extraction and quantification of polyglucans*
173 Leaves were harvested at the end of the day, immediately frozen in liquid nitrogen
174 and stored at - 80°C until use. Two different protocols were then applied for polyglucan
175 extraction.
176 Isolation of insoluble polyglucans (for microscopy and crystallographic analysis) was
177 adapted from (Streb *et al.*, 2008). Several tens of grams of leaves were homogenized in a
178 buffered medium (0.1 M Na-acetate (pH 4.8); 0.05% Triton X-100, 2 mM EDTA) with a
179 blender, and then filtered on two layers of Miracloth (Calbiochem). SDS was added to the
180 filtrate at a final concentration of 1.5% (w/v) and the insoluble polyglucans were collected
181 by centrifugation (20 min at 20,000 g). Then, the samples were washed 4 times with water

and were sequentially filtered on nylon meshes of decreasing pore size, in the order: 100, 31 and 11 µm. The filtrates were centrifuged (10 min at 16,000 g) and the polyglucan pellet was resuspended in 20% ethanol and stored at 4°C until use.

Extraction of insoluble and soluble polyglucans (for quantification and ultrastructure analysis) was performed on 1 g of leaves using the perchloric acid method described in detail in (Streb *et al.*, 2008).

The polyglucan content was measured by a spectrophotometric method (Enzytec™, R-BIOPHARM®) following the manufacturer's instructions.

*Analysis of the ultrastructure of polyglucans*

The chain length distribution (CLD) of the polyglucans was determined with 200 µg of purified material debranched with a mix of 4 U isoamylase (*Pseudomonas sp.*, Megazyme) and 2U pullulanase (*Klebsiella planticola*, Megazyme) in sodium acetate buffer (55 mM final concentration, pH3.5) incubated overnight at 42°C in a final volume of 500 µL. After 10 min at 100°C, the mix was desalted on Alltech™ Extract-Clean™ Carbograph columns (Fisher Scientific). First, columns were equilibrated with 5 mL of 25% acetonitrile and washed with 5 mL of deionized sterile water. Then, samples were loaded on the columns and subsequently rinsed with 5ml of deionized water. Sample elution was performed with 2 mL of 25% acetonitrile. The samples were lyophilized and resuspended in 250 µL of deionized water. The chain length distribution of each sample was determined by HPAEC-PAD analysis (Dionex® – PA200 CarboPac column) as fully described in (Roussel *et al.*, 2013).

205 *Starch fractionation*

206 Starch fractionation (separation of high and low mass polymers) was performed by
207 size exclusion chromatography on a Sepharose CL-2B matrix. 1.2 mg of starch was
208 dispersed in 200 µL of DMSO (100%) during 15 min at 100 °C. The polymers were
209 precipitated by the addition of 800µL of absolute ethanol. After centrifugation for 5 min at
210 10,000 g, the pellet was solubilized in 500 µL of 10 mM NaOH and loaded onto the column
211 previously equilibrated with 10 mM NaOH (0.5 cm i.d. × 65 cm) at a flow rate of 12 $mL.h^{-1}$
212 [1]. Fractions of 300 µL were collected and the glucans were detected using $I_2$ / KI solution
213 (0.1% and 1% w/v respectively).

214

215 *Protein extraction*

216 Protein extracts were obtained from approximately 1 g of fresh leaves harvested at the
217 middle of the day and directly frozen in liquid nitrogen. Frozen leaves were finely
218 powdered and immersed in ice-cold 100 mM Tricine/KOH (pH 7.8) 5 mM $MgCl_2$, 1 mM
219 DTT containing 0.1 % of protease inhibitor cocktail (ProteaseArrest™, G Biosciences).
220 Samples were centrifuged at 16,000 g at 4°C during 10 min. The supernatant was collected
221 and the protein content was determined by Bradford assay.

222

223 *Zymogram of branching enzyme activity*

224 Zymograms of branching enzyme activity were obtained according to the method
225 described by (Tetlow *et al.*, 2004; Tetlow *et al.*, 2008). Branching enzyme activity is
226 detected indirectly by the stimulation of phosphorylase « a ». In the presence of a high

227 concentration of Glc-1-P and the absence of Pi, phosphorylase « a » synthesizes linear
228 α(1→4)-linked polyglucans that can be branched in α(1→6) if a branching enzyme is in the
229 vicinity. Branching increases the number of available non-reducing ends and thus
230 stimulates phosphorylase « a » polymerizing activity. This leads to the synthesis of
231 branched polyglucans that can be detected in the form of dark brown bands in the gel after
232 iodine staining. In brief, 5% polyacrylamide resolving gel was prepared with 0.2 $U.mL^{-1}$ of
233 rabbit phosphorylase « a » (Sigma), 0.1% (w/v) of maltoheptaose (Sigma) and 0.1% (w/v)
234 of acarbose (Sigma-Aldrich). 60 µg of proteins were mixed with loading buffer in a 20:1
235 ratio (loading buffer: 2 $mg.mL^{-1}$ of bromophenol blue and 50% (v/v) glycerol) and loaded
236 onto the gel. After migration (1 h 30 min at 15 $V.cm^{-1}$), the gel was washed twice in 0.4%
237 MES (w/v) and 2.9% sodium citrate (w/v). After incubation for 2 h at 30°C in 0.4% MES
238 (w/v) and 2.9% sodium citrate (w/v) supplemented with 1.4% of glucose-1-phosphate
239 (w/v), 0.09% adenosine monophosphate (w/v), 0.15% EDTA (w/v) and 0.06% DTT (w/v),
240 the gel was revealed with $I_2$/KI solution (0.1% / 1% (w/v)).
241
242 In vitro *assay of branching enzyme activity*
243 The branching enzyme activity in leaf extracts was determined according to the
244 method described in details by (Tetlow *et al.*, 2008).
245
246 *Western blotting*
247 Protein extracts were treated as for zymogram analysis described above. After
248 migration, proteins were transferred to a nitrocellulose membrane (Whatmann) with a
249 transfer buffer (0.025 M Tris; 0.192 M glycine; 20% (v/v) methanol). After transfer the

membrane was incubated in a blocking solution (0.01 M Tris; 0.25 M NaCl, 1.5% (w/v) BSA) during 15 min and then incubated overnight with the primary antibody diluted at 1/5000 in the blocking solution at room temperature. Then the membrane was washed three times in TTBS (0.1 M Tris; 0.25 M NaCl; 0.1% (v/v) Tween 20). The membrane was incubated for 2 h with a 1/30000 dilution of the secondary antibody (anti-rabbit IgG-alkaline phosphatase; Sigma) at room temperature. The membrane was finally rinsed three times with TTBS buffer and developed with the BCIP/NTB substrate kit following manufacturer's instructions (Invitrogen).

The primary antibody raised against GlgB was produced in rabbit by the inoculation of a peptide specific of the *E. coli* branching enzyme (Eurogentec). Peptide sequence: $NH_2$-NLYEHSDPREGYHQDW -$CONH_2$ (position 355-370 of *E. coli* GlgB protein); Protein carrier: KLH.

*Transmission and scanning electron microscopy*

Strips of freshly cut leaves harvested at the end of the day were fixed with glutaraldehyde, post-fixed with osmium tetroxide and embedded in Epon resin. 70 nm-thin sections were cut with a diamond knife in a Leica UC6 microtome and post-stained with periodic acid thiosemicarbazide silver proteinate (PATAg) (Gallant *et al.*, 1997). Drops of dilute suspensions of purified glucans were deposited on glow-discharged coated copper grids and the preparations were negatively stained with 2% uranyl acetate. All specimens were observed with a Philips CM200 transmission electron microscope (TEM) operating at 80 kV. Images were recorded on Kodak SO163 films. In addition, drops of suspensions of purified glucans were allowed to dry on freshly cleaved mica and coated with Au/Pd. The

specimens were observed with a Jeol JSM6300 scanning electron microscope (SEM) operating at 8 kV and secondary electron images were recorded using the SIS ADDA II system.

*Wide-angle X-ray scattering*

The crystallinity index of the polyglucan samples was measured by wide-angle X-ray scattering following a method described by (Wattebled *et al.*, 2008).

## RESULTS

### *Selection of Arabidopsis lines expressing GlgB*

*glgB* from *E. coli* was fused downstream of the nucleotide sequence encoding AtBE2 (At5g03650) chloroplast transit peptide. The resulting cDNA was then cloned into pMDC32, a binary vector designed for transgene expression under the control of the CaMV 35S promoter. *be2 be3* double mutants were transformed by the floral dip method (Clough *et al.*, 1998) with an *Agrobacterium tumefaciens* strain carrying the construct. Among 6000 plants tested, 98 transformants (T1), displaying hygromycin resistance, were selected on MS agar plates. 5 independent homozygous lines were selected among their progeny (T2 plants) and further analyzed for their leaf iodine-staining phenotype (Figure 1). At the end of the daytime period, while wild-type (WT) leaves stain black due to normal amounts of starch, *be2 be3* leaves stain yellow because they lack polysaccharides. By contrast, *isa1 isa3 pu1* leaves stain orange because they accumulate high amounts of phytoglycogen (Wattebled *et al.*, 2008). The phenotypes of the transformants, called “β lines”, were

296 intermediate between those of WT and *isa1 isa3 pu1* lines, suggesting that the
297 polysaccharide synthesis was at least partially restored. However, while β20 and β6 lines
298 stain brown, β12 stains dark brown and β1 stains dark grey, suggesting different levels of
299 complementation. β5 is noteworthy since iodine staining is not homogeneous in that line. A
300 grey stain was observed at the apex of some leaves, while other leaves remained yellow. It
301 suggests a non-homogeneous expression of the transgene in that line. For clarity, only β1,
302 β12, and β20 lines, that are representative of each phenotype, will be further presented here.
303 Results obtained for lines β5 and β6 are available as Supporting figures (Figure S6; Figure
304 S7 and Figure S8).

305 The *be2 be3* double mutant displays strong growth retardation probably due to the
306 over-accumulation of maltose (Dumez *et al.*, 2006). Therefore, we analyzed the
307 developmental phenotype of the transformants as well as *be2 be3* and wild-type plants
308 (Figure S2). Contrary to *be2 be3* mutant plants, GlgB-expressing lines were similar to the
309 wild type at maturity.

310

311 ***Expression and activity of GlgB***

312 The expression of GlgB in the "β" lines was confirmed by western blot using a
313 peptide-specific anti-*E. coli* BE antibody raised against a 16-mer peptide of the protein
314 (Figure 2A). As expected, while GlgB is absent in *be2 be3* and WT, a unique band of
315 approximately 85 kDa was observed in the transgenic lines. Interestingly, each of these
316 lines displays increasing band intensity in the order: β1, β12 and β20. Zymograms of BE
317 activity were obtained using cell extracts prepared from leaves harvested at the middle of
318 the light period (Figure 2B). As already described (Dumez *et al.*, 2006), no BE activity is

observed in the *be2 be3* mutant of Arabidopsis while WT displays one band of activity on the zymogram (Figure 2B). In contrast, a large activity band of lower mobility was found in the *E. coli* extract. BE electrophoretic profiles of the transgenic lines differ between each other as well as from those of *E. coli* and Arabidopsis. Indeed, one band of intermediate mobility (Figure 2B, a + b) is present in all extracts of the three "β" lines (Figure 2B). Moreover, an additional band with a higher mobility than that of Arabidopsis BE is visible in line β20 (Figure 2B, c). Band intensities also vary among "β" lines, being far greater in β12 and β20 extracts compared to β1 (Figure 2B).

Correlations between zymogram activities and *glgB* expression in the transgenic lines were sought by western blot. Leaf or cell protein extracts were separated by polyacrylamide gel electrophoresis in non-denaturing conditions similar to those used in the zymogram assay. As expected, no cross-reaction could be seen in *Arabidopsis* WT and *be2 be3* samples. One band was observed in the *E. coli* extract, the mobility of which corresponded to the activity detected on the zymogram (Figure 2B and 2C). Similarly, two bands corresponding to the activities observed on the zymogram were visible in the β1, β12, and β20 transgenic lines (Figure 2C, a and b). However, the intensity of the two bands in line β1 was lower than that of the two other transgenic lines. A third band of higher mobility was also clearly visible in line β20 (Figure 2C, c) and may correspond to the high mobility activity observed on the zymogram.

Zymogram and immunoblotting assays suggest that different levels of BE activity can be found in the lines tested in this work. Thus, BE activity was measured *in vitro* by the phosphorylase « a » stimulating assay using $^{14}$C-labeled Glc-1-P (Figure 2D). Leaf extracts were incubated for 10, 20 or 40 min at 30°C and Glc-1-P consumption was plotted against

342 the incubation time (Figure 2D). This assay confirmed that BE activity increased in the "β"
343 lines, in the order: β1, β12 and β20. An extremely low level of activity was detected in the
344 *be2 be3* mutant of Arabidopsis (phosphorylase « a » activity is not stimulated because of
345 the lack of BE activity in this line) while WT shows significant incorporation of Glc into
346 polyglucan after 40 min of incubation.
347
348 ***Polyglucan accumulation in the glgB expressing lines***
349 Iodine-staining phenotypes of the transgenic lines expressing *glgB* suggest that starch
350 and/or water-soluble polysaccharide synthesis is at least partially restored despite the lack
351 of endogenous branching enzymes. These polyglucans were assayed after extraction from
352 leaves harvested at the end of the 16-h light period (Figure 3). Wild-type Arabidopsis plants
353 accumulate insoluble polysaccharides and only tiny amounts of non-methanol-precipitable
354 sugars (i.e. glucose and maltooligosaccharides), while methanol-precipitable
355 polysaccharides could not be detected (Figure 3). Interestingly, line β1 displayed the
356 highest amount of insoluble polyglucans among transgenic lines while it also showed the
357 lowest BE activity (Figure 2 and Figure 3). In line with this, insoluble polysaccharide
358 contents were lower in both β12 and β20, in contrast to the levels of BE activity observed
359 in these plants. Interestingly, methanol-precipitable glucans were detected at significant
360 levels in β12 and β20 compared to β1. Finally, non-methanol-precipitable glucans were
361 found at a relatively high level in β20 (about 1 $mg.g^{-1}$ of fresh leaves) compared to the
362 other lines (0.35 $mg.g^{-1}$ in β12; 0.2 $mg.g^{-1}$ in β1; 0.05 $mg.g^{-1}$ in WT). Note that in the same
363 culture conditions (16 h light), the *be2 be3* double mutant accumulated very high amounts
364 of maltose (up to 20 $mg.g^{-1}$ of fresh weight) (Dumez *et al.*, 2006).

365

366 ***Observation of polyglucans accumulation in leaf chloroplasts***

367 The accumulation of polyglucans was directly observed *in planta* by transmission
368 electron microscopy (TEM - Figure 4). Ultrathin sections of leaves were observed after
369 positive staining of the polyglucans with PATAg. Flat and smooth starch granules of
370 approximately 1-3 µm were observed in WT (Figure 4A), as already described in the
371 literature. By contrast, no starch granules were detected in the *be2 be3* double mutant, in
372 agreement with the phenotype already described for this line (Figure 4B) (Dumez *et al.*,
373 2006). The *isa1 isa3 pu1* triple mutant was included in this analysis as a starchless
374 phytoglycogen-accumulating line. Phytoglycogen was visible in the form of very small and
375 polydisperse particles homogeneously distributed in the stroma of the chloroplasts (Figure
376 4C). Different types of particles were observed in the three lines expressing *glgB*. Lines β1
377 and β12 accumulated 0.2 - 3 µm-large and irregularly shaped particles (Figure 4D and 4E,
378 respectively), while β20 contained significantly smaller and highly polydisperse particles
379 (Figure 4F). The larger objects could reach 1 µm in size but most particles were smaller
380 than 0.2 µm. The image of β20 is thus similar to that of *isa1 isa3 pu1* (Figure 4C) although
381 no large aggregates were observed in the images of the triple DBE mutant. The surface of
382 the particles was irregular and rather rough in β1 while it was smoother in β12. In both
383 specimens, the fact that the larger particles may correspond to the aggregation of smaller
384 units cannot be excluded.

385

386 ***Morphology of purified insoluble and soluble polyglucans***

387 The insoluble polyglucans were also observed by scanning electron microscopy
388 (SEM) after extraction from leaves and purification (Figure 5). In WT, starch granules
389 appeared as individual flat particles with a smooth surface, as usually observed for
390 Arabidopsis starch granules (Figure 5A). Their size ranged between 1 and 4 µm. The
391 identification of individual particles in extracts from the transgenic lines was very difficult,
392 and aggregates or particle networks were generally observed (Figure 5B-5D). This
393 artefactual aggregation may be due to the repeated centrifugations performed during the
394 polyglucan purification and/or a reconcentration upon drying on the supporting mica.
395 Nevertheless, despite this aggregation, constituting units could be recognized within the
396 particle networks in each image and their size clearly decreased with increasing GlgB
397 activity, in agreement with the TEM observation of ultrathin sections of leaves (Figure 4D-
398 4F).

399 Higher resolution images of the insoluble polyglucans were recorded by TEM of
400 negatively stained preparations. As the particles extracted from β1 were too large to be
401 observed with this technique, only particles extracted from β12 and β20 are shown in
402 Figure 6. Moreover, only the smallest of these insoluble particles could be properly stained
403 and observed in sufficient detail. Consequently, the images illustrate the morphology of this
404 fraction of particles but may not represent that of the larger objects.

405 The insoluble polyglucans in β12 often appeared as aggregates of smaller particles
406 with various shape and size (Figure 6A and 6B). 200 nm bulky and rather smooth
407 spheroidal particles could be recognized, often in contact with multilobular less well-
408 defined material. The particles in β20 are more flat and exhibit a clear multilobular aspect

(Figure 6C and 6D). Their average size is still around a few hundreds nanometers but they seem to be composed of 50-70 nm subunits. Although it is difficult to see if the larger particles are aggregates of individual subunits formed upon centrifugation and/or drying, the morphology resembles that of the so-called α-particles observed in liver glycogen and constituted of smaller β-subunits (Ryu *et al.*, 2009; Sullivan *et al.*, 2012).

TEM images of the polyglucans isolated from the soluble fractions from β12 and β20 are shown in Figure 7. In both cases, 20-30 nm particles are observed (Figure 7A and 7B) whose aspect and size distribution are very similar to those of maize phytoglycogen (Figure 7C).

***Ultrastructure of insoluble and soluble polyglucans***

The ultrastructure of insoluble and soluble polyglucans was determined and compared to that of reference samples. First, insoluble polyglucans were fractionated by size exclusion chromatography on Sepharose CL-2B® (Figure 8). WT starch shows a regular elution profile exhibiting two peaks (Figure 8A). The first peak corresponds to high-mass amylopectin (between 10 and 13 mL) while the second broader peak corresponds to the low-mass amylose (between 16 and 27 mL). The elution profile of insoluble polyglucans for line β1 also contains two distinct peaks corresponding to high-mass (same elution volume as WT amylopectin) and low-mass material (elution volume equivalent to that of WT amylose), respectively (Figure 8B). However, the peak of low-mass material is much higher and slightly shifted towards lower masses (to the right on the diagram) compared to WT amylose. Moreover, the $\lambda_{max}$ of the iodine-polysaccharide complex for high-mass

material in line β1 is 10 nm higher compared to that of WT amylopectin. This suggests that this material is composed, on average, of longer-chain glucans than WT amylopectin. β12 and β20 insoluble polyglucans display more or less the same elution profile (Figure 8C and 8D, respectively). A unique large peak of high-mass material is observed, the elution profile of which is equivalent to that of WT amylopectin. Contrary to WT and β1 insoluble polyglucans, no distinct peak of low-mass material was seen in β12 and β20 lines. In addition, the $\lambda_{max}$ of the high-mass material in these two lines was decreased by 10 nm compared to WT amylopectin, suggesting that the length of the glucans is shorter on average (Table1).

The crystallinity index of the insoluble polyglucans was determined by wide-angle X-ray scattering. The analyses were performed on two samples of polyglucans extracted from two plant preparations cultivated independently (Table 1). All samples are of B-type allomorph. The WT starch granules have a crystallinity index of 33%, in agreement with previous reports on Arabidopsis starch (Wattebled *et al.*, 2008). The β1 and β12 insoluble polyglucans display a lower crystallinity index (27 and 20%, respectively), while the β20 insoluble glucans have the lowest crystallinity index (13%) among those analyzed in this work.

The chain length distribution (CLD) profile of the insoluble polyglucans was established after debranching with a mixture of bacterial isoamylase and pullulanase. The resulting linear glucans were separated and quantified by HPAEC-PAD (Figure 9). The profile of β1 polyglucans has a DP max of 12-13 glucosyl residues identical to WT starch (Figure 9A and 9C). However, the fraction of DP 5-18 glucans is higher and the fraction of DP 21-40 is lower in β1 compared to WT. The higher fraction of short glucans (DP<13)

454 that do not interact with iodine may explain the increase of the $\lambda_{max}$ of the iodine-
455 polyglucan complex observed in this sample (Table 1). The β12 insoluble polyglucan has a
456 profile similar to that of β1 although the fraction of DP 5-11 glucans is higher, especially at
457 DP 6-7 (Figure 9A). In β20, the $DP_{max}$ is at DP 7 and the profile strongly resembles that of
458 the insoluble glucan synthesized by the *Arabidopsis isa1 isa3 pu1* triple mutant (Figure 9B)
459 apart from for a strong depletion of DP 3-4 glucans in β20 that is probably due to the
460 presence of DBE activity in that line compared to the triple DBE mutant.

461 The branching degree of the insoluble polyglucans was estimated according to the
462 method described in (Szydlowski *et al.*, 2011) (Table 1). WT, β1, β12 and β20 polyglucans
463 had branching degrees of 5.1, 6.1, 6.8 and 7.3%, respectively. The branching degree of the
464 phytoglycogen of the *Arabidopsis isa1 isa3 pu1* triple mutant was estimated at 8.1%, a
465 value very close to that previously reported (Szydlowski *et al.*, 2011).

466 The CLD profiles were also established for the soluble polyglucans isolated from the
467 transgenic lines. The corresponding profiles were compared to that of rabbit liver glycogen
468 (Figure S3). In all cases, DP 7 chains were the most abundant among those analyzed.
469 Although the profiles of the transgenic lines were all similar, they were different to that of
470 glycogen with a significant excess of DP 5-13 chains and a deficit in DP > 17 chains.

471

472 **DISCUSSION**

473 About 20 years ago, it was suggested that isoamylase-type debranching enzymes
474 (DBEs) were required for the building of the final structure of amylopectin in plants,
475 determining insolubility and partial crystallization (Ball *et al.*, 1996; Mouille *et al.*, 1996;
476 Myers *et al.*, 2000). This idea was further supported and confirmed by several studies

conducted with different plant species (James *et al.*, 1995; Nakamura, 1996; Rahman *et al.*, 1998; Delatte *et al.*, 2005; Wattebled *et al.*, 2005). In all cases, the lack of isoamylase-type DBEs (except the ISA3 isoform dedicated to starch degradation) caused a strong reduction of starch accumulation, and a modification of the ultrastructure of the residual starch accompanied by a decrease of the crystallinity index. Moreover, these isoamylase mutants also accumulate phytoglycogen, a water-soluble and amorphous glucan structure, which is comparable to that of the glycogen found in animals, fungi and bacteria. However, the synthesis of high amounts of insoluble polyglucans was reported in a quintuple mutant of Arabidopsis lacking all four DBEs plus one form of plastidial α-amylase (Streb *et al.*, 2008). Thus, the necessity of DBEs *per se* for the determination of the water-insolubility and crystallinity of starch could be questioned, although the polyglucans synthesized in the above-mentioned quintuple mutant displays specific features (very high DP<10 content for instance) not observed in WT starch. Therefore, the function of branching enzymes (BEs) appears to be crucial in establishing the intrinsic structural features of starch although crystallinity of the polyglucan synthesized in the Arabidopsis quintuple mutant was not reported in (Streb *et al.*, 2008). To test this hypothesis, we have substituted *A. thaliana* starch branching enzymes (BE2 and BE3), main contributors to the synthesis of starch in leaves, with the *E. coli* glycogen branching enzyme (GlgB) and the synthesis of polyglucans was investigated. The suppression of both BE2 and BE3 in *Arabidopsis* resulted in the complete loss of starch branching enzyme activity (Figure 2B and 2D) and the loss of starch synthesis and was accompanied by the accumulation of maltose and plant growth retardation (Dumez *et al.*, 2006). Other starch metabolizing enzymes were not affected by the mutations. Thus, the *be2 be3* double mutant represents an excellent model

500 to investigate the ability of GlgB to restore starch or starch-like polyglucan synthesis in
501 Arabidopsis.

502 The expression of *glgB* in *A. thaliana* was successfully achieved after
503 transformation of the corresponding cDNA into *be2 be3* plants. The corresponding protein
504 was detected by immunoblot analysis of leaf extracts of several independently transformed
505 plants (Figures 2A and 2C) and the branching activity of the enzyme was also detected
506 (Figures 2B and 2D). Different levels of expression were obtained, although all plants
507 analyzed in this study were homozygous for the transgene. Indeed, the level of BE activity
508 was much higher in β20 compared to β12, and most notably compared to β1 which had the
509 lowest BE activity as measured by zymogram and *in vitro* radioactive assay (Figures 2B
510 and 2D). These levels of activity were correlated with GlgB protein contents. Immunoblot
511 analysis performed under denaturing or non-denaturing conditions (Figures 2A and 2C
512 respectively) showed that the content of GlgB is higher in β20 than in β12 and even more
513 than in β1, which is in good agreement with the level of activity assayed in each line.
514 Interestingly, immunoblot analysis performed under non-denaturing conditions (Figure 2C)
515 revealed several bands reacting with the anti-GlgB antibody in the transgenic lines. Two
516 major bands (Figure 2B bands a and b) were detected in all three lines and a third band
517 (Figure 2B band c) of higher mobility but lower intensity was specifically observed in β20.
518 Two additional lines were analyzed during this work: β5 and β6. Corresponding results are
519 presented as Supporting data in the form of Figures S6, S7 and S8 and confirm the results
520 presented above. Line β5, which has a very low GlgB activity, displays a phenotype similar
521 to that of β1. Conversely line β6, that has high GlgB activity, is similar to β20. This result

522 suggests that GlgB is either post-translationally modified when expressed in *Arabidopsis* or
523 is involved in the formation of protein complexes (homo or heteromeric complexes) with
524 different electrophoretic mobility (Tetlow *et al.*, 2004; Makhmoudova *et al.*, 2014).

525 Although GlgB was expressed and active in all transgenic lines, the phenotype of
526 polyglucan accumulation was different from one line to another. Indeed, albeit displaying
527 the lowest GlgB expression level, β1 accumulated polyglucans with a structure close to that
528 of WT starch. These polyglucans had a granular morphology and individual particles were
529 observed in the stroma of the chloroplast (Figure 4). These granules had a size similar to
530 that of WT starch although their surface appeared to be rougher. Smaller PATAg-stained
531 particles, with a size well below 1 µm, were also dispersed throughout the stroma of β1
532 chloroplasts. Moreover, the β1 insoluble polyglucan fraction was partially crystalline (27%
533 compared to 33% for WT starch) and was composed of both high-mass amylopectin-like
534 material and low-mass amylose-like material (Figure 8). Further, the CLD profile after
535 debranching was similar to that of WT starch although it was enriched in DP 5-19 chains
536 (with a $DP_{max}$ at 12 glucose residues such as in WT starch) and depleted in DP 21-40 chains
537 (Figure 9). As a whole, the β1 polyglucan can be considered as starch-like implying that a
538 bacterial glycogen BE can sustain the synthesis of such specifically ordered polysaccharide
539 when expressed in plants. It follows that the final distribution of the branch points within
540 starch and consequently the properties of the synthesized polyglucan (crystallinity, water-
541 insolubility, granular morphology, amylopectin $DP_{max}$ at 12-13, and the presence of
542 amylose) is not solely under the control of starch branching enzymes (although branching
543 enzyme activity is mandatory to create α(1→6) linkages). Otherwise, expression of a

544 bacterial glycogen-branching enzyme in the plant would have resulted in the synthesis of
545 soluble and amorphous glycogen-like polymers. Nevertheless, the polyglucan that
546 accumulates in β1 can not be regarded as true WT starch and several hypotheses can be
547 proposed which could explain why this is the case. Firstly, GlgB is expressed in
548 *Arabidopsis* under the control of the constitutive 35S promoter. Consequently, GlgB is
549 likely expressed linearly during the day and the night, which may influence the final
550 structure of the synthesized polyglucan. However, the expression of the endogenous BEs
551 (BE2 and BE3) is not strongly correlated with the day/night cycle (Smith *et al.*, 2004).
552 Indeed, BE2 exhibits only slightly higher expression in the day compared to the night. BE3,
553 expression is significantly higher during the day compared to night and displays an
554 expression pattern that resembles that of enzymes involved in starch degradation (Smith *et*
555 *al.*, 2004), although, more recently, BE3 protein abundance was reported as unmodified
556 throughout the day/night cycle (Skeffington *et al.*, 2014). The second hypothesis relies to
557 the intrinsic properties of GlgB activity. Indeed, starch BE isoforms have different catalytic
558 properties (Tetlow, 2012). In *A. thaliana*, in contrast to other plants and to other dicots,
559 only class-II branching enzymes (BE2 and BE3) have been described so far. However,
560 because of its catalytic properties, GlgB can be classified in the class-I plant branching
561 enzymes and preferentially transfers DP 6-15 chains (with a maximum for DP 10-12
562 chains) (Guan *et al.*, 1997; Sawada *et al.*, 2014). Therefore it is not surprising that the
563 expression of a class-I BE instead of class-II BEs results in modifications in the structure of
564 the synthesized polysaccharide compared to the wild type. Another explanation relates to
565 enzyme complex formation. It is now well established that some of the starch metabolizing
566 enzymes interact to form hetero-multimeric complexes (Hennen-Bierwagen *et al.*, 2008;

567 Tetlow *et al.*, 2008; Hennen-Bierwagen *et al.*, 2009). Branching enzymes are important
568 components of these complexes as shown in the endosperm of cereals (Liu *et al.*, 2009; Liu
569 *et al.*, 2012a; Liu *et al.*, 2012b). Although it has not been shown yet, it is likely that starch-
570 metabolizing enzymes also organize in the form of multisubunit complexes in Arabidopsis.
571 It is highly probable that BE2/BE3 and GlgB are engaged in different protein complexes or
572 simply that GlgB is unable to interact with other endogenous plant enzymes. This could
573 result in the modification of other starch-metabolizing activities and consequently
574 polyglucan structure. Even if enzymes of starch synthesis do not physically interact in
575 Arabidopsis chloroplasts, their activities must still be interdependent in order to produce the
576 final structure of amylopectin. Removing one or several enzymes of the pathway could alter
577 the activity of others whose normal activity depends on the presence of the complete set of
578 enzymes (Szydlowski *et al.*, 2011; Nakamura *et al.*, 2012; Abe *et al.*, 2014; Brust *et al.*,
579 2014; Nakamura *et al.*, 2014). GlgB may only partially counterbalance the lack of both
580 BE2 and BE3 in the transgenic lines, which, in turn, may alter other starch-metabolizing
581 activities. Lastly, some starch-metabolizing enzymes are regulated by the redox state of the
582 cell or the organelle where the pathway occurs (Glaring *et al.*, 2012; Lepisto *et al.*, 2013). It
583 is possible that GlgB does not behave like Arabidopsis BEs which are redox sensitive
584 (Glaring *et al.*, 2012), thus modifying the branching activity in the transgenic lines and
585 explaining why it is not possible to restore a true WT phenotype.

586 Finally, it should be emphasized that the ability to form starch-like structures
587 depends on the level of branching enzyme activity of GlgB. Indeed, β20, which possessed
588 the highest GlgB activity, synthesizes polyglucans whose structure resembles more or less

589 that of the residual insoluble glucans isolated from Arabidopsis DBE mutants (Wattebled *et*
590 *al.*, 2008). The β12 line, that had a GlgB activity intermediate between that of β1 and β20,
591 displays an intermediate polyglucan-accumulating phenotype. Debranching enzyme activity
592 level was estimated in the different lines by zymogram analysis (Figure S4). No obvious
593 modification of isoamylase activity was detected in the GlgB-expressing plants compared
594 to the wild type. Starch synthase activity was also evaluated with zymograms (Figure S5).
595 SS1 and SS3 are the two major isoforms of starch synthases encompassing over 90% of the
596 elongating activity measured in *Arabidopsis* leaf extracts (Szydlowski *et al.*, 2011). Starch
597 synthase activities were unmodified in the *be2 be3* mutant (Dumez *et al.*, 2006). Both SS1
598 and SS3 activities were reduced in β1 compared to WT. The activity of SS1 was slightly
599 higher in β12 and β20 compared to WT whereas SS3 was, to some extent, reduced. At this
600 stage it is unclear why starch synthase activity is modified in the transgenic lines, especially
601 in β1. Nevertheless, despite possessing the lowest starch synthase activity, β1 is the GlgB
602 expressing line accumulating the highest amount of insoluble polyglucans. Thus the
603 remaining SS activity in β1 appears in be in excess of that needed to allow the synthesis of
604 the insoluble polyglucan, and does not seem to be a limiting factor.

605 Thus, in a context of non-limiting starch synthase activity, the accumulation of the
606 insoluble and soluble polyglucans in β20 occurs under circumstances of over-branching
607 which cannot be balanced by the debranching activity of endogenous isoamylases and
608 pullulanase. This results in a higher branching degree (7.3%) and a very low crystallinity
609 index (13%) of the insoluble polyglucans in β20. Such increase of the branching degree of
610 the polyglucan produced in plants after the expression of *E. coli* GlgB has already been

611 described in potato and rice (Kortstee *et al.*, 1996; Kim *et al.*, 2005). In both cases, the
612 number of branch points of amylopectin was significantly increased. However, because
613 endogenous BE activity was not knocked down in these plants the actual contribution of
614 GlgB for the synthesis of the highly branched starch was impossible to determine.

615 Our result suggests that a finely tuned balance between branching and debranching
616 activities is probably acting *in planta* to control α(1→6) linkage placement and number,
617 and consequently to allow the formation of starch or starch-like polyglucan. Figure 10 is an
618 attempt to model our interpretation of the results generated in this work. As a model, it is
619 likely a simplified view of reality (for instance starch synthases are not included in the
620 model) and was conceptualized from the results of the expression of a bacterial enzyme in
621 plants. However, we suggest that it could be generalized to any situation where the balance
622 between BE and DBE activity is compromised. For instance, in rice, the endogenous BEIIb
623 isoform was expressed in a BEIIb-defective mutant by expression of the corresponding
624 structural gene (Tanaka *et al.*, 2004). Overexpression of the protein and of the
625 corresponding activity was obtained in one of the transgenic lines leading to the
626 accumulation of significantly higher amount of soluble polyglucan compared to the wild
627 type (almost three times more). This was accompanied by enrichment in DP<15 glucans of
628 amylopectin and alteration of the crystalline structure of starch.

629 Nevertheless expression of GlgB did not restore the synthesis of true WT starch,
630 possibly because GlgB activity cannot be regulated in the same way as endogenous BEs.
631 Protein complexes and thus other enzyme activities (starch synthases for instance) might be

632 affected by the lack of endogenous BEs, leading to the synthesis of structurally modified
633 polyglucan as frequently observed in mutants defective for enzymes of the pathway.

## ACKNOWLEDGEMENTS

The authors thank Dr. Nicolas Szydlowski for fruitful discussions and critical reading of the manuscript, and gratefully acknowledge the financial support of Agence Nationale de la Recherche (contract # ANR-11-BSV6-0003) and the Natural Sciences and Engineering Research Council of Canada (Team Discovery Grant, number 435781, MJE, IJT).

640 **REFERENCES**

641

642 Abe N., Asai H., Yago H., Oitome N., Itoh R., Crofts N., . . . Fujita N. (2014) Relationships
643 between starch synthase I and branching enzyme isozymes determined using double
644 mutant rice lines. *BMC Plant Biology*, **14**, 80.
645 Ball S., Guan H.-P., James M., Myers A., Keeling P., Mouille G., . . . Preiss J. (1996) From
646 Glycogen to Amylopectin: A Model for the Biogenesis of the Plant Starch Granule.
647 *Cell*, **86**, 349-352.
648 Ball S.G. & Morell M.K. (2003) From bacterial glycogen to starch: understanding the
649 biogenesis of the plant starch granule. *Annu Rev Plant Biol*, **54**, 207-233.
650 Bertoft E. (2004) On the nature of categories of chains in amylopectin and their connection
651 to the super helix model. *Carbohydrate Polymers*, **57**, 211-224.
652 Bertoft E. (2013) On the building block and backbone concepts of amylopectin structure.
653 *Cereal Chemistry*, **90**, 294-311.
654 Brust H., Lehmann T., D'Hulst C. & Fettke J. (2014) Analysis of the functional interaction
655 of Arabidopsis starch synthase and branching enzyme isoforms reveals that the
656 cooperative action of SSI and BEs results in glucans with polymodal chain length
657 distribution similar to amylopectin. *PLoS One*, **9**, e102364.
658 Buleon A., Colonna P., Planchot V. & Ball S. (1998) Starch granules: structure and
659 biosynthesis. *International Journal of Biological Macromolecules*, **23**, 85-112.

660 Burton R.A., Bewley J.D., Smith A.M., Bhattacharyya M.K., Tatge H., Ring S., . . . Martin
661 C. (1995) Starch branching enzymes belonging to distinct enzyme families are
662 differentially expressed during pea embryo development. *Plant J*, **7**, 3-15.
663 Clough S.J. & Bent A.F. (1998) Floral dip: a simplified method for Agrobacterium-
664 mediated transformation of Arabidopsis thaliana. *Plant J*, **16**, 735-743.
665 Delatte T., Trevisan M., Parker M.L. & Zeeman S.C. (2005) Arabidopsis mutants *Atisa1*
666 and *Atisa2* have identical phenotypes and lack the same multimeric isoamylase,
667 which influences the branch point distribution of amylopectin during starch
668 synthesis. *Plant J*, **41**, 815-830.
669 Dumez S., Wattebled F., Dauvillée D., Delvallé D., Planchot V., Ball S.G. & D'Hulst C.
670 (2006) Mutants of Arabidopsis lacking starch branching enzyme II substitute
671 plastidial starch synthesis by cytoplasmic maltose accumulation. *Plant Cell*, **18**,
672 2694-2709.
673 Facon M., Lin Q., Azzaz A.M., Hennen-Bierwagen T.A., Myers A.M., Putaux J.L., . . .
674 Wattebled F. (2013) Distinct functional properties of isoamylase-type starch
675 debranching enzymes in monocot and dicot leaves. *Plant Physiol*, **163**, 1363-1375.
676 Fisher D.K., Gao M., Kim K.N., Boyer C.D. & Guiltinan M.J. (1996) Two closely related
677 cDNAs encoding starch branching enzyme from Arabidopsis thaliana. *Plant Mol*
678 *Biol*, **30**, 97-108.
679 Fujita N. & Nakamura Y. (2012) Distinct and overlapping functions of starch synthase
680 isoforms. In: *Starch: Origins, Structure and Metabolism.* (ed I.J. Tetlow), pp. 115-
681 140. Society for Experimental Biology, London, UK.

682 Gallant D.J., Bouchet B. & Baldwin P.M. (1997) Microscopy of starch: evidence of a new
683 level of granule organization. *Carbohydrate Polymers*, **32**, 177-191.
684 Glaring M.A., Skryhan K., Kotting O., Zeeman S.C. & Blennow A. (2012) Comprehensive
685 survey of redox sensitive starch metabolising enzymes in Arabidopsis thaliana.
686 *Plant Physiol Biochem*, **58**, 89-97.
687 Guan H., Kuriki T., Sivak M. & Preiss J. (1995) Maize branching enzyme catalyzes
688 synthesis of glycogen-like polysaccharide in glgB-deficient Escherichia coli. *Proc*
689 *Natl Acad Sci U S A*, **92**, 964-967.
690 Guan H., Li P., Imparl-Radosevich J., Preiss J. & Keeling P. (1997) Comparing the
691 Properties of *Escherichia coli* Branching Enzyme and Maize Branching Enzyme.
692 *Archives of Biochemistry and Biophysics*, **342**, 92-98.
693 Guan H.P., Baba T. & Preiss J. (1994) Expression of branching enzyme I of maize
694 endosperm in Escherichia coli. *Plant Physiol.*, **104**, 1449-1453.
695 Guan H.P. & Preiss J. (1993) Differentiation of the properties of the branching isozymes
696 from maize (Zea mays). *Plant Physiol*, **102**, 1269-1273.
697 Harrison S.J., Mott E.K., Parsley K., Aspinall S., Gray J.C. & Cottage A. (2006) A rapid
698 and robust method of identifying transformed Arabidopsis thaliana seedlings
699 following floral dip transformation. *Plant Methods*, **2**, 19.
700 Hennen-Bierwagen T.A., Lin Q., Grimaud F., Planchot V., Keeling P.L., James M.G. &
701 Myers A.M. (2009) Proteins from multiple metabolic pathways associate with
702 starch biosynthetic enzymes in high molecular weight complexes: a model for
703 regulation of carbon allocation in maize amyloplasts. *Plant Physiol*, **149**, 1541-
704 1559.

705 Hennen-Bierwagen T.A., Liu F., Marsh R.S., Kim S., Gan Q., Tetlow I.J., . . . Myers A.M.
706 (2008) Starch biosynthetic enzymes from developing maize endosperm associate in
707 multisubunit complexes. *Plant Physiol*, **146**, 1892-1908.
708 Hizukuri S. (1986) Polymodal distribution of the chain lengths of amylopectins, and its
709 significance. *Carbohydrate Research*, **147**, 342-347.
710 Huang X.-F., Nazarian-Firouzabadi F., Vincken J.-P., Ji Q., Suurs L.C.J.M., Visser R.G.F.
711 & Trindade L.M. (2013) Expression of an engineered granule-bound Escherichia
712 coli glycogen branching enzyme in potato results in severe morphological changes
713 in starch granules. *Plant Biotechnology Journal*, **11**, 470-479.
714 James M.G., Robertson D.S. & Myers A.M. (1995) Characterization of the maize gene
715 sugary1, a determinant of starch composition in kernels. *Plant Cell*, **7**, 417-429.
716 Jyothishwaran G., Kotresha D., Selvaraj T., Srideshikan S.M., Rajvanshi P.K. &
717 Jayabaskaran C. (2007) A modified freeze-thaw method for efficient transformation
718 of Agrobacterium tumefaciens. *Current Science*, **93**, 770-772.
719 Kim W.S., Kim J., Krishnan H.B. & Nahm B.H. (2005) Expression of Escherichia coli
720 branching enzyme in caryopses of transgenic rice results in amylopectin with an
721 increased degree of branching. *Planta*, **220**, 689-695.
722 Kortstee A.J., Vermeesch A.M., de Vries B.J., Jacobsen E. & Visser R.G. (1996)
723 Expression of *Escherichia coli* branching enzyme in tubers of amylose-free
724 transgenic potato leads to an increased branching degree of the amylopectin. *Plant*
725 *J*, **10**, 83-90.
726 Lepisto A., Pakula E., Toivola J., Krieger-Liszkay A., Vignols F. & Rintamaki E. (2013)
727 Deletion of chloroplast NADPH-dependent thioredoxin reductase results in inability

728 to regulate starch synthesis and causes stunted growth under short-day
729 photoperiods. *J Exp Bot*, **64**, 3843-3854.
730 Liu F., Ahmed Z., Lee E.A., Donner E., Liu Q., Ahmed R., . . . Tetlow I.J. (2012a) Allelic
731 variants of the amylose extender mutation of maize demonstrate phenotypic
732 variation in starch structure resulting from modified protein-protein interactions. *J*
733 *Exp Bot*, **63**, 1167-1183.
734 Liu F., Makhmoudova A., Lee E.A., Wait R., Emes M.J. & Tetlow I.J. (2009) The amylose
735 extender mutant of maize conditions novel protein-protein interactions between
736 starch biosynthetic enzymes in amyloplasts. *J Exp Bot*, **60**, 4423-4440.
737 Liu F., Romanova N., Lee E.A., Ahmed R., Evans M., Gilbert E.P., . . . Tetlow I.J. (2012b)
738 Glucan affinity of starch synthase IIa determines binding of starch synthase I and
739 starch-branching enzyme IIb to starch granules. *Biochem J*, **448**, 373-387.
740 Makhmoudova A., Williams D., Brewer D., Massey S., Patterson J., Silva A., . . . Emes
741 M.J. (2014) Identification of multiple phosphorylation sites on maize endosperm
742 starch branching enzyme IIb, a key enzyme in amylopectin biosynthesis. *J Biol*
743 *Chem*, **289**, 9233-9246.
744 Melendez-Hevia E., Waddell T.G. & Shelton E.D. (1993) Optimization of molecular design
745 in the evolution of metabolism: the glycogen molecule. *Biochem J*, **295 ( Pt 2)**, 477-
746 483.
747 Mouille G., Maddelein M.L., Libessart N., Talaga P., Decq A., Delrue B. & Ball S. (1996)
748 Preamylopectin processing: a mandatory step for starch biosynthesis in plants. *Plant*
749 *Cell*, **8**, 1353-1366.

750 Myers A.M., Morell M.K., James M.G. & Ball S.G. (2000) Recent progress toward
751 understanding biosynthesis of the amylopectin crystal. *Plant Physiol*, **122**, 989-997.
752 Nakamura Y. (1996) Some properties of starch debranching enzymes and their possible
753 role in amylopectin biosynthesis. *Plant Science*, **121**, 1-18.
754 Nakamura Y., Aihara S., Crofts N., Sawada T. & Fujita N. (2014) In vitro studies of
755 enzymatic properties of starch synthases and interactions between starch synthase I
756 and starch branching enzymes from rice. *Plant Sci*, **224**, 1-8.
757 Nakamura Y., Ono M., Utsumi C. & Steup M. (2012) Functional interaction between
758 plastidial starch phosphorylase and starch branching enzymes from rice during the
759 synthesis of branched maltodextrins. *Plant Cell Physiol*, **53**, 869-878.
760 Pfister B., Lu K.J., Eicke S., Feil R., Lunn J.E., Streb S. & Zeeman S.C. (2014) Genetic
761 evidence that chain length and branch point distributions are linked determinants of
762 starch granule formation in Arabidopsis. *Plant Physiol*, **165**, 1457-1474.
763 Rahman A., Wong K., Jane J., Myers A.M. & James M.G. (1998) Characterization of SU1
764 isoamylase, a determinant of storage starch structure in maize. *Plant Physiol*, **117**,
765 425-435.
766 Roach P.J., Depaoli-Roach A.A., Hurley T.D. & Tagliabracci V.S. (2012) Glycogen and its
767 metabolism: some new developments and old themes. *Biochem J*, **441**, 763-787.
768 Roussel X., Lancelon-Pin C., Vikso-Nielsen A., Rolland-Sabate A., Grimaud F., Potocki-
769 Veronese G., . . . D'Hulst C. (2013) Characterization of substrate and product
770 specificity of the purified recombinant glycogen branching enzyme of
771 Rhodothermus obamensis. *Biochim Biophys Acta*, **1830**, 2167-2177.

772 Ryu J.H., Drain J., Kim J.H., McGee S., Gray-Weale A., Waddington L., . . . Stapleton D.
773 (2009) Comparative structural analyses of purified glycogen particles from rat liver,
774 human skeletal muscle and commercial preparations. *Int J Biol Macromol*, **45**, 478-
775 482.
776 Satoh H., Nishi A., Yamashita K., Takemoto Y., Tanaka Y., Hosaka Y., . . . Nakamura Y.
777 (2003) Starch-Branching Enzyme I-Deficient Mutation Specifically Affects the
778 Structure and Properties of Starch in Rice Endosperm. *Plant Physiol.*, **133**, 1111-
779 1121.
780 Sawada T., Nakamura Y., Ohdan T., Saitoh A., Francisco P.B., Jr., Suzuki E., . . . Ball S.
781 (2014) Diversity of reaction characteristics of glucan branching enzymes and the
782 fine structure of alpha-glucan from various sources. *Arch Biochem Biophys*, **562**, 9-
783 21.
784 Schwall G.P., Safford R., Westcott R.J., Jeffcoat R., Tayal A., Shi Y.-C., . . . Jobling S.A.
785 (2000) Production of very-high-amylose potato starch by inhibition of SBE A and
786 B. *Nat Biotech*, **18**, 551-554.
787 Seo B.S., Kim S., Scott M.P., Singletary G.W., Wong K.S., James M.G. & Myers A.M.
788 (2002) Functional interactions between heterologously expressed starch-branching
789 enzymes of maize and the glycogen synthases of Brewer's yeast. *Plant Physiol*, **128**,
790 1189-1199.
791 Skeffington A.W., Graf A., Duxbury Z., Gruissem W. & Smith A.M. (2014) Glucan, Water
792 Dikinase Exerts Little Control over Starch Degradation in Arabidopsis Leaves at
793 Night. *Plant Physiology*, **165**, 866-879.

794 Smith S.M., Fulton D.C., Chia T., Thorneycroft D., Chapple A., Dunstan H., . . . Smith
795 A.M. (2004) Diurnal Changes in the Transcriptome Encoding Enzymes of Starch
796 Metabolism Provide Evidence for Both Transcriptional and Posttranscriptional
797 Regulation of Starch Metabolism in Arabidopsis Leaves. *Plant Physiol.*, **136**, 2687-
798 2699.
799 Streb S., Delatte T., Umhang M., Eicke S., Schorderet M., Reinhardt D. & Zeeman S.C.
800 (2008) Starch granule biosynthesis in Arabidopsis is abolished by removal of all
801 debranching enzymes but restored by the subsequent removal of an endoamylase.
802 *Plant Cell*, **20**, 3448-3466.
803 Sullivan M.A., O'Connor M.J., Umana F., Roura E., Jack K., Stapleton D.I. & Gilbert R.G.
804 (2012) Molecular insights into glycogen alpha-particle formation.
805 *Biomacromolecules*, **13**, 3805-3813.
806 Szydlowski N., Ragel P., Hennen-Bierwagen T.A., Planchot V., Myers A.M., Merida A., . .
807 . Wattebled F. (2011) Integrated functions among multiple starch synthases
808 determine both amylopectin chain length and branch linkage location in Arabidopsis
809 leaf starch. *J Exp Bot*, **62**, 4547-4559.
810 Tanaka N., Fujita N., Nishi A., Satoh H., Hosaka Y., Ugaki M., . . . Nakamura Y. (2004)
811 The structure of starch can be manipulated by changing the expression levels of
812 starch branching enzyme IIb in rice endosperm. *Plant Biotechnology Journal*, **2**,
813 507-516.
814 Tetlow I.J. (2012) Branching enzymes and their role in determining structural and
815 functional properties of polyglucans. In: *Starch: Origins, Structure and Metabolism.*
816 (ed I.J. Tetlow), pp. 141-178. Society for Experimental Biology, London, UK.

817 Tetlow I.J., Beisel K.G., Cameron S., Makhmoudova A., Liu F., Bresolin N.S., . . . Emes
818 M.J. (2008) Analysis of protein complexes in wheat amyloplasts reveals functional
819 interactions among starch biosynthetic enzymes. *Plant Physiol*, **146**, 1878-1891.
820 Tetlow I.J., Wait R., Lu Z., Akkasaeng R., Bowsher C.G., Esposito S., . . . Emes M.J.
821 (2004) Protein phosphorylation in amyloplasts regulates starch branching enzyme
822 activity and protein-protein interactions. *Plant Cell*, **16**, 694-708.
823 Wattebled F., Dong Y., Dumez S., Delvalle D., Planchot V., Berbezy P., . . . D'Hulst C.
824 (2005) Mutants of Arabidopsis lacking a chloroplastic isoamylase accumulate
825 phytoglycogen and an abnormal form of amylopectin. *Plant Physiol*, **138**, 184-195.
826 Wattebled F., Planchot V., Dong Y., Szydlowski N., Pontoire B., Devin A., . . . D'Hulst C.
827 (2008) Further evidence for the mandatory nature of polysaccharide debranching for
828 the aggregation of semicrystalline starch and for overlapping functions of
829 debranching enzymes in Arabidopsis leaves. *Plant Physiol*, **148**, 1309-1323.
830 Yao Y., Thompson D.B. & Guiltinan M.J. (2004) Maize Starch-Branching Enzyme
831 Isoforms and Amylopectin Structure. In the Absence of Starch-Branching Enzyme
832 IIb, the Further Absence of Starch-Branching Enzyme Ia Leads to Increased
833 Branching. *Plant Physiol.*, **136**, 3515-3523.
834

## TABLES

**Table 1:** The branching degree was calculated according to (Szydlowski *et al.*, 2011). The $\lambda_{max}$ of the iodine-amylopectin complex was determined after insoluble polyglucans fractionation by SEC on CL-2B matrix (Figure 8). It was determined at the fraction of maximum absorbance. The crystallinity index and allomorph were determined by wide-angle X-ray scattering. All samples were of B-type. The values are the means of two independent assays. In the case of the *isa1 isa3 pu1* triple mutant, the branching degree was determined for phytoglycogen. NA = not available.

| Sample | WT | β1 | β12 | β20 | *isa1 isa3 pu1* |
|---|---|---|---|---|---|
| Branching degree (%) | 5.1 | 6.1 | 6.8 | 7.3 | 8.1 |
| $\lambda_{max}$ of amylopectin (nm) | 563 | 572 | 553 | 552 | NA |
| Crystallinity index (%) | 33 | 27 | 20 | 13 | NA |

## FIGURE LEGENDS

**Figure 1: Iodine staining of individual plants harvested at the end of the day.** 2-week old plants were harvested and stained with iodine solution after being destained in hot ethanol. All pictures are at the same scale. Colors and intensity of the stain is indicative of the polyglucan content and structure. Wild-type (WT) plants stain dark brown because of the synthesis of high amount of normal starch (ecotype *Wassilewkija*). The *be2 be3* plants stain yellow as a consequence of the lack of any polyglucan in this mutant (Dumez *et al.*, 2006). *isa1 isa3 pu1* is a debranching enzyme triple mutant accumulating high amount of phytoglycogen (Wattebled *et al.*, 2008) and therefore stains orange with iodine. β1, β5, β6, β12 and β20 are hygromycin resistant plants selected after transformation of the *be2 be3* mutant with a vector containing the *E. coli glgB* gene. Intermediate colors between those of the WT and the *isa1 isa2* mutant were obtained suggesting that polyglucan synthesis is partially restored in these transgenic lines.

**Figure 2: Expression of glgB in the *be2 be3* transformed lines.** (A) Immunoblot analysis performed in denaturing conditions. Protein extracts were denatured before and during migration in the polyacrylamide gel. After migration, proteins were blotted onto a nitrocellulose membrane and hybridized with a peptide-directed antibody raised against GlgB. (B) zymogram of branching enzyme activity. The polyacrylamide gel contains DP7 maltooligosaccharides and phosphorylase “a”. Branching enzyme activity was revealed by incubating the gel for 2 hours in a phosphorylase “a” stimulating buffer. Bands of branched polyglucans were detected by soaking the gel in iodine solution. (C) Immunoblot analysis performed in non-denaturing conditions: protein extract preparation and migration in the

867 gel was carried out as in (B). After migration, proteins were treated as in (A). WT: wild
868 type of *A. thaliana* (*Wassilewskija* ecotype); β1, β12, β20: transgenic plants expressing
869 GlgB; *be2 be3*: branching enzyme double mutant (Dumez *et al.*, 2006); *E. coli*: bacterial
870 cell extract of wild type *E. coli*. Proteins or activity bands corresponding to GlgB expressed
871 in plants were labelled as a, b, and c. In (A), (B) and (C) all lines are from the same gel and
872 blots. (D) *in vitro* assay of branching enzyme activity. Protein extracts were incubated for
873 10 to 40 min in a buffer containing DP7 maltooligosaccharides, phosphorylase "a" and [U-
874 $^{14}$C]Glc-1-P (7.4 kBq per assay) at 50 mM final concentration. The mean of incorporated
875 Glc into branched polyglucans was calculated for 3 independent assays and plotted against
876 the time of incubation. Vertical lines stand for standard deviation. Open diamonds: WT
877 extract; closed squares: *be2 be3* mutant; closed circles: β1; open squares: β12; open circles:
878 β20.

879 **Figure 3: Leaf glucan contents.** Glucans were extracted from leaves of 3-week old
880 plants by the perchloric acid protocol. Leaves were harvested at the end of 16-h light
881 period. Insoluble and soluble polyglucans and sugars/maltooligosaccharides were assayed
882 by a spectrophotometric method. The averages of three independent cultures are presented.
883 WT: wild type *WS* ecotype; β1, β12, β20: transgenic plants expressing the *E. coli glgB*
884 gene. Vertical thin bars are the standard deviation of three independent biological
885 replicates.

886 **Figure 4: Transmission electron microscopy of leaf chloroplasts.** Leaves from
887 plants were harvested at the end of the day, cut in small strips and immediately fixed with
888 glutaraldehyde in a cacodylate buffer and stained with PATAg to reveal glucans. A: wild

889 type from *Wassilewskija* ecotype of *A. thaliana*; B: *be2 be3*: branching enzyme double
890 mutant; C: *isa1 isa3 pu1*: debranching enzyme triple mutant accumulating phytoglycogen
891 (Wattebled *et al.*, 2008); D: β1, E: β12, F: β20: *be2 be3* transgenic plants expressing the
892 bacterial *glgB* gene.

893 **Figure 5: Scanning electron microscopy of purified insoluble polyglucans.**
894 Insoluble polyglucans were extracted and purified from leaves of 3-week-old plants
895 harvested at the end of the day of 16-h light / 8-h dark cycles. A: wild type *Wassilewskija*
896 ecotype; B: β1; C: β12; D: β20.

897 **Figure 6: Morphology of particles purified from the insoluble polyglucans of**
898 **the GlgB-expressing lines.** TEM images of negatively stained particles from the insoluble
899 fractions of β12 (A, B) and β20 (C, D).

900 **Figure 7: Morphology of particles purified from the soluble polyglucans**
901 **isolated from the GlgB-expressing lines.** TEM images of negatively stained particles
902 from the water-soluble polyglucans isolated from β12 (A) and β20 (B). The image of maize
903 phytoglycogen (C) is given for comparison.

904 **Figure 8: Fractionation of insoluble polyglucans by size exclusion**
905 **chromatography.** Purified insoluble polyglucans were dispersed in DMSO, solubilized in
906 NaOH 10 mM and loaded onto a Sepharose® CL-2B matrix. Elution was conducted in
907 NaOH 10 mM at a rate of 12 $mL.h^{-1}$. 300 µL fractions were collected and subsequently
908 analyzed by iodine spectrophotometry. Thick continuous lines are the maximum
909 absorbance of the iodine-polyglucan complexes (left Y-axis). Dashed lines indicate the

910 wavelength (nm) of the iodine-polyglucan complex at the maximum of absorbance (right
911 Y-axis). X-axis is the volume of elution in mL. A: WT; B: β1; C: β12; D: β20.

912 **Figure 9: Chain length distribution of insoluble polyglucans.** Purified insoluble
913 polyglucans were digested with a mix of bacterial debranching enzymes. The
914 corresponding linear glucans were separated by high-performance anion exchange
915 chromatography and detected by pulsed amperometric detection (HPAEC-PAD). The
916 fraction of each DP (from 3 to 60 glucose residues) is expressed in % of the total DP
917 presented on the profile. (A) WT: continuous black line; β1: grey triangles; β12: closed
918 circles; β20: discontinuous grey line. (B) Comparison of the profiles of the WT (continuous
919 black line) and β20 (discontinuous grey line). The profile of the *isa1 isa3 pu1* triple mutant
920 already published in (Wattebled *et al.*, 2008) is given (open diamonds). (C) Comparison of
921 the profiles of the WT (continuous black line) and β1 (grey triangles).

922 **Figure 10: Starch or starch-like polyglucan synthesis occurs thanks to a**
923 **balanced branching / debranching activity ratio assuming that starch synthase**
924 **activity is not limiting whatever the branching/debranching ratio.** Left panel: in the
925 absence of branching activity (*be2 be3* double mutant), starch or phytoglycogen synthesis is
926 impossible and is substituted by maltose accumulation; the BR/DEBR ratio is null. Middle
927 panel: when the ratio BR/DEBR activity is balanced (WT) or near-balanced (β1), starch or
928 starch-like polyglucan synthesis is promoted. In the case of β1, the slight structural
929 modification of starch is due to the expression of the bacterial glycogen-branching enzyme
930 that has different catalytic and regulatory properties. Right panel: in the absence of
931 debranching activity (such as in *isa1 isa3 pu1*; BR/DEBR is infinite) or when branching

932 activity is extremely high (such as in β20; BR/DEBR >> optimal) phytoglycogen or
933 phytoglycogen-like insoluble polyglucan is synthesized respectively. Superimposed
934 drawings correspond to (from left to right): maltose, amylopectin, phytoglycogen; black
935 points depict the reducing end.

936

# SUPPORTING INFORMATION

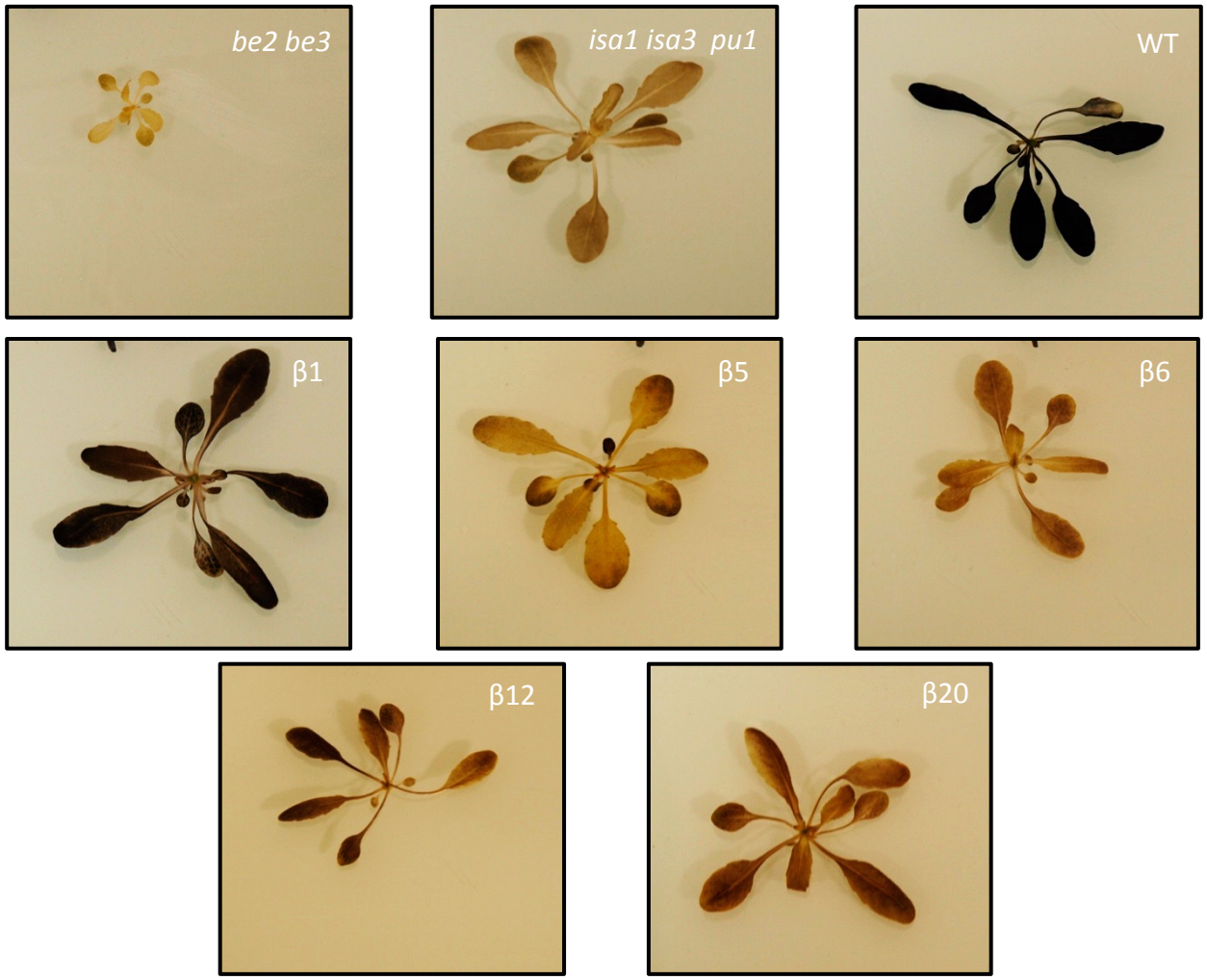


**Figure 1: Iodine staining of individual plants harvested at the end of the day.** 2-week old plants were harvested and stained with iodine solution after being destained in hot ethanol. All pictures are at the same scale. Colors and intensity of the stain is indicative of the polyglucan content and structure. Wild-type (WT) plants stain dark brown because of the synthesis of high amount of normal starch (ecotype *Wassilewkija*). The *be2 be3* plants stain yellow as a consequence of the lack of any polyglucan in this mutant (Dumez et al. 2006). *isa1 isa3 pu1* is a debranching enzyme triple mutant accumulating high amount of phytoglycogen (Wattebled et al. 2008) and therefore stains orange with iodine. β1, β5, β6, β12 and β20 are hygromycin resistant plants selected after transformation of the *be2 be3* mutant with a vector containing the *E. coli glgB* gene. Intermediate colors between those of the WT and the *isa1 isa2* mutant were obtained suggesting that polyglucan synthesis is partially restored in these transgenic lines.

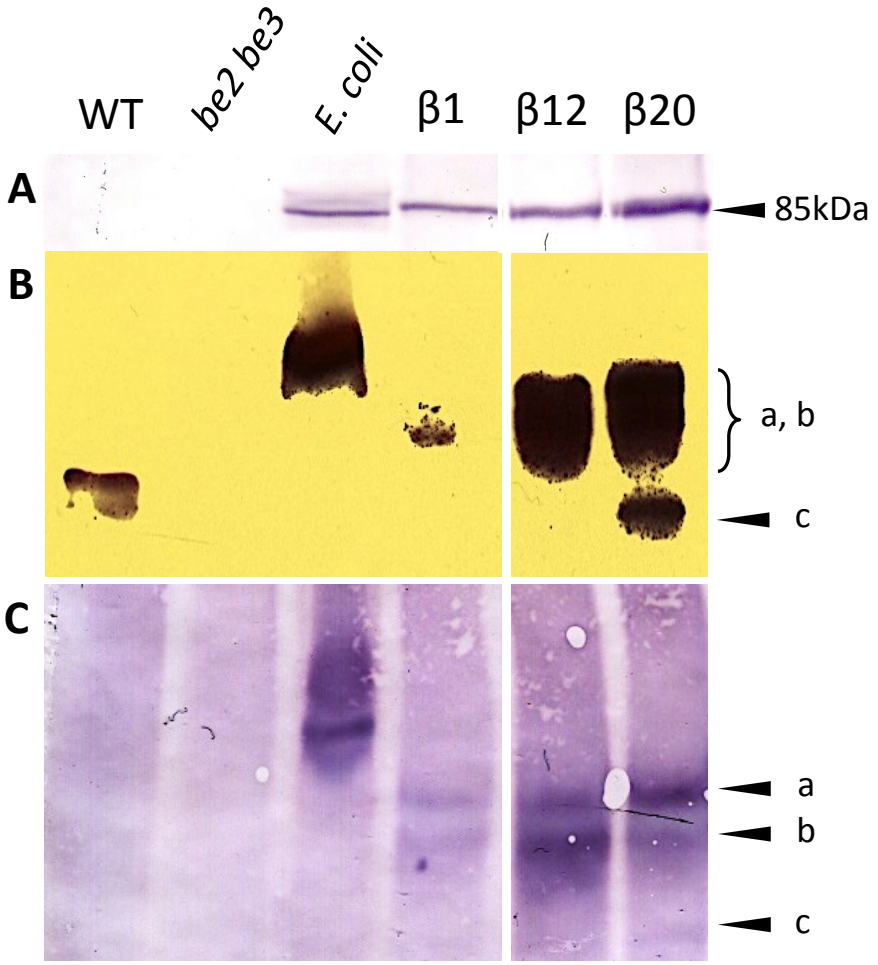


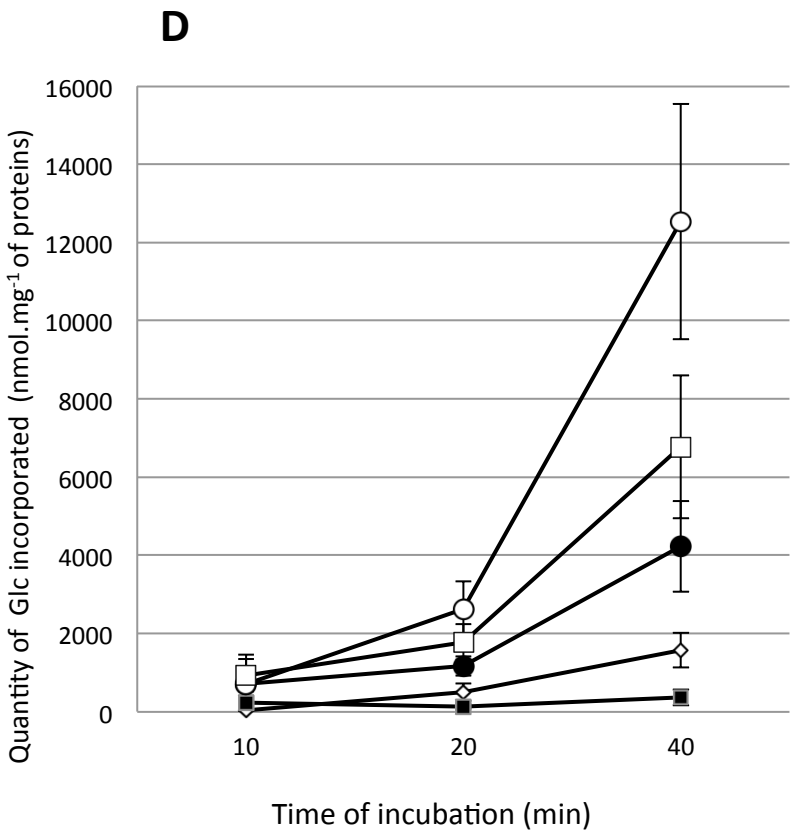


**Figure 2: Expression of glgB in the *be2 be3* transformed lines.** (A) Immunoblot analysis performed in denaturing conditions. Protein extracts were denatured before and during migration in the polyacrylamide gel. After migration, proteins were blotted onto a nitrocellulose membrane and hybridized with a peptide-directed antibody raised against GlgB. (B) zymogram of branching enzyme activity. The polyacrylamide gel contains DP7 maltooligosaccharides and phosphorylase "a". Branching enzyme activity was revealed by incubating the gel for 2 hours in a phosphorylase "a" stimulating buffer. Bands of branched polyglucans were detected by soaking the gel in iodine solution. (C) Immunoblot analysis performed in non-denaturing conditions: protein extract preparation and migration in the gel was carried out as in (B). After migration, proteins were treated as in (A). WT: wild type of *A. thaliana* (*Wassilewskija* ecotype); β1, β12, β20: transgenic plants expressing GlgB; *be2 be3*: branching enzyme double mutant (Dumez et *al*., 2006); *E. coli*: bacterial cell extract of wild type *E. coli*. Proteins or activity bands corresponding to GlgB expressed in plants were labeled as a, b , and c. In (A), (B) and (C) all lines are from the same gel and blots. (D) *in vitro* assay of branching enzyme activity. Protein extracts were incubated for 10 to 40 min in a buffer containing DP7 maltooligosaccharides, phosphorylase "a" and [U-$^{14}$C]Glc-1-P (7.4 kBq per assay) at 50 mM final concentration. The mean of incorporated Glc into branched polyglucans was calculated for 3 independent assays and plotted against the time of incubation. Vertical lines stand for standard deviation. Open diamonds: WT extract; closed squares: *be2 be3* mutant; closed circles: β1; open squares: β12; open circles: β20.

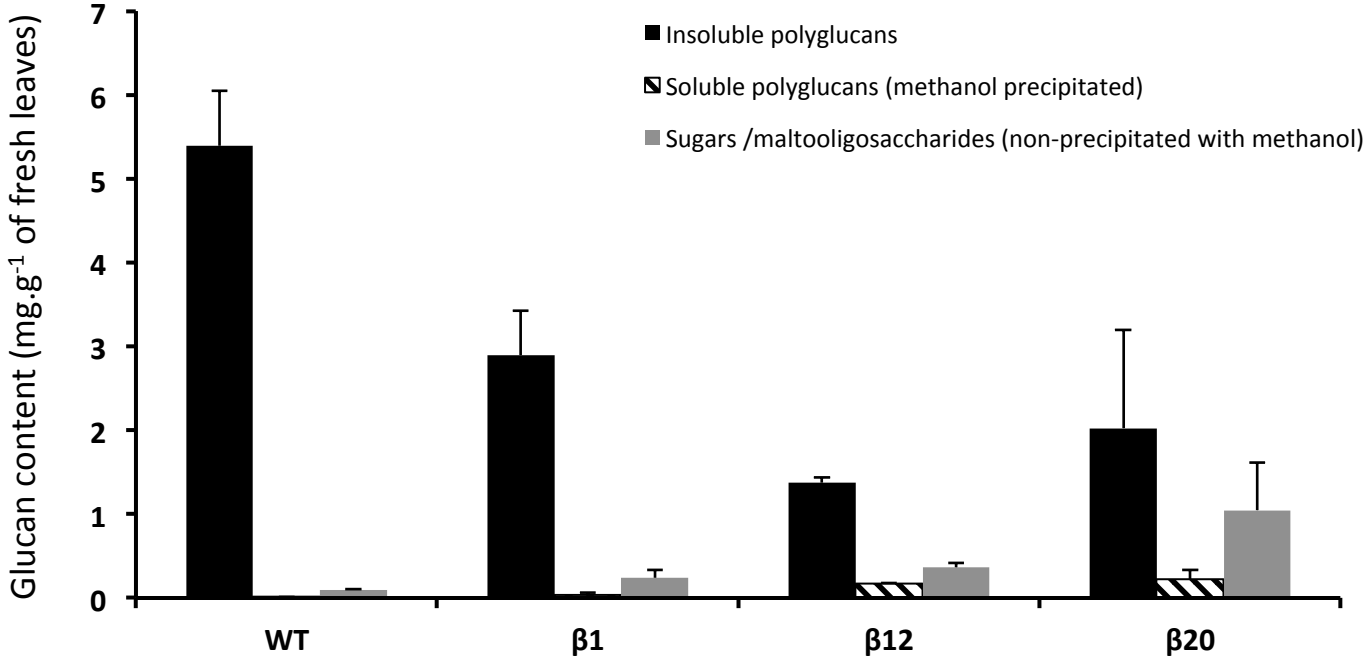


**Figure 3: Leaf glucan contents.** Glucans were extracted from leaves of 3-week old plants by the perchloric acid protocol. Leaves were harvested at the end of 16-h light period. Insoluble and soluble polyglucans and sugars/ maltooligosaccharides were assayed by a spectrophotometric method. The averages of three independent cultures are presented. WT: wild type *WS* ecotype; β1, β12, β20: transgenic plants expressing the *E. coli glgB* gene. Vertical thin bars are the standard deviation of three independent biological replicates.

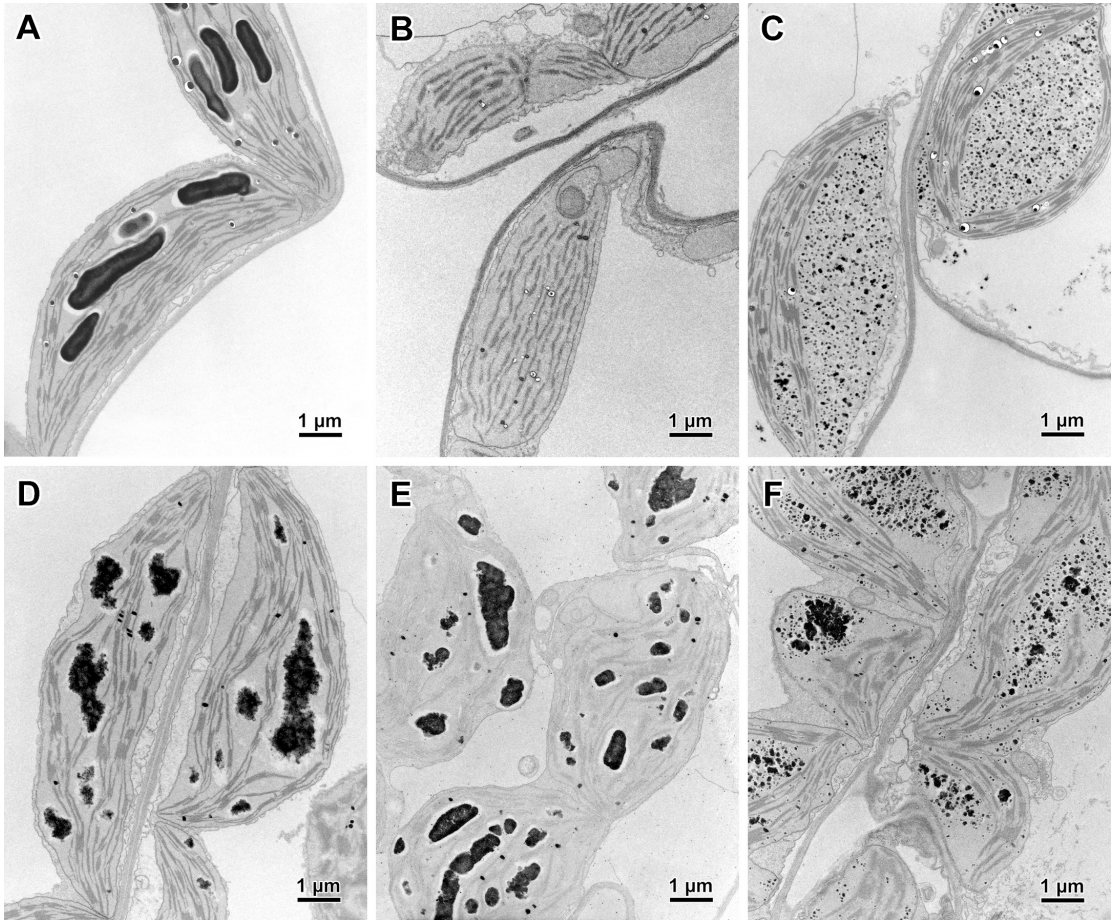


**Figure 4: Transmission electron microscopy of leaf chloroplasts.** Leaves from plants were harvested at the end of the day, cut in small strips and immediately fixed with glutaraldehyde in a cacodylate buffer and stained with PATAg to reveal glucans. A: wild type from *Wassilewskija* ecotype of *A. thaliana*; B: *be2 be3*: branching enzyme double mutant; C: *isa1 isa3 pu1*: debranching enzyme triple mutant accumulating phytoglycogen (Wattebled et al. 2008); D: β1, E: β12, F: β20: *be2 be3* transgenic plants expressing the bacterial *glgB* gene.

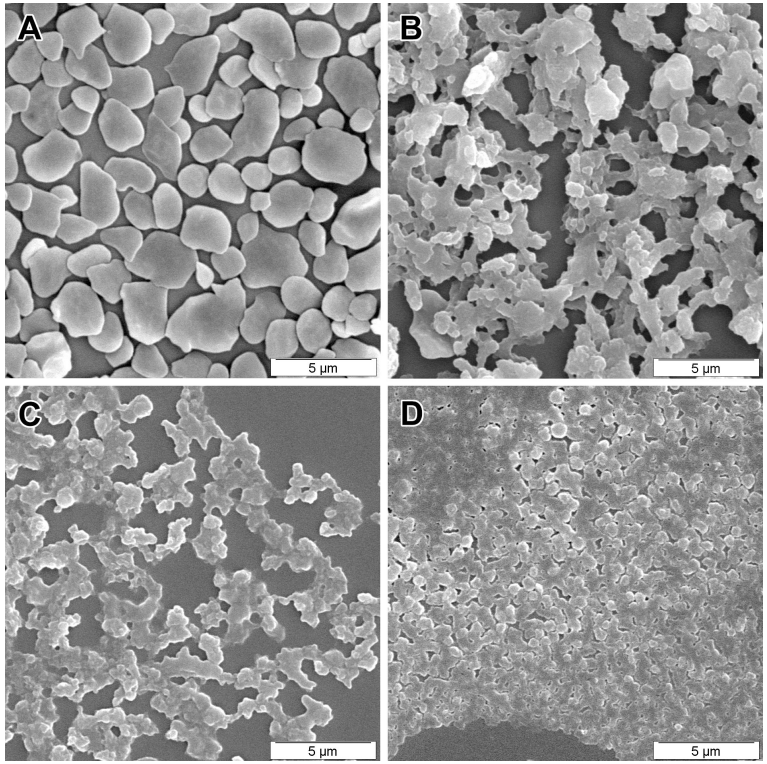


**Figure 5: Scanning electron microscopy of purified insoluble polyglucans.** Insoluble polyglucans were extracted and purified from leaves of 3-week-old plants harvested at the end of the day of 16-h light / 8-h dark cycles. A: wild type *Wassilewskija* ecotype; B: β1; C: β12; D: β20.

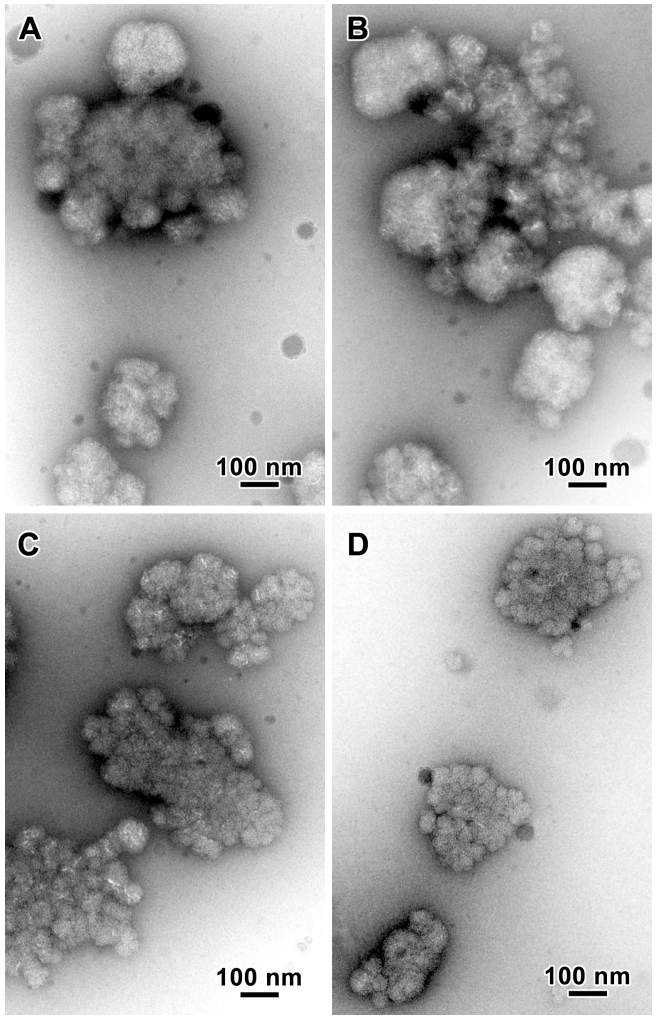


**Figure 6: Morphology of particles purified from the insoluble polyglucans of the GlgB-expressing lines.** TEM images of negatively stained particles from the insoluble fractions of β12 (A, B) and β20 (C, D).

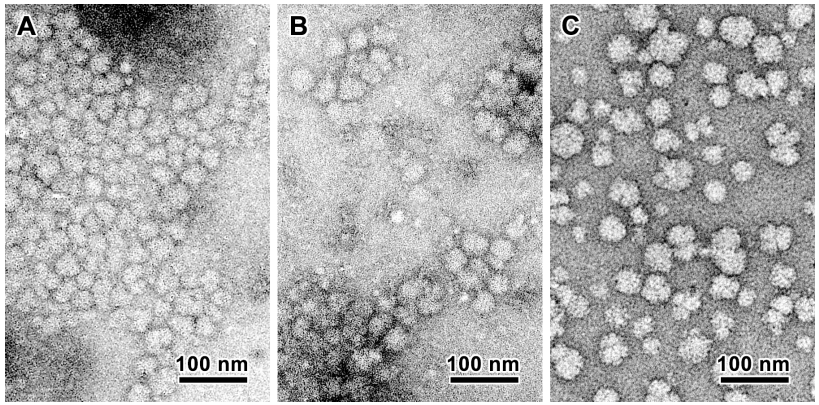


**Figure 7: Morphology of particles purified from the soluble polyglucans isolated from the GlgB-expressing lines.** TEM images of negatively stained particles from the water-soluble polyglucans isolated from β12 (A) and β20 (B). The image of maize phytoglycogen (C) is given for comparison.

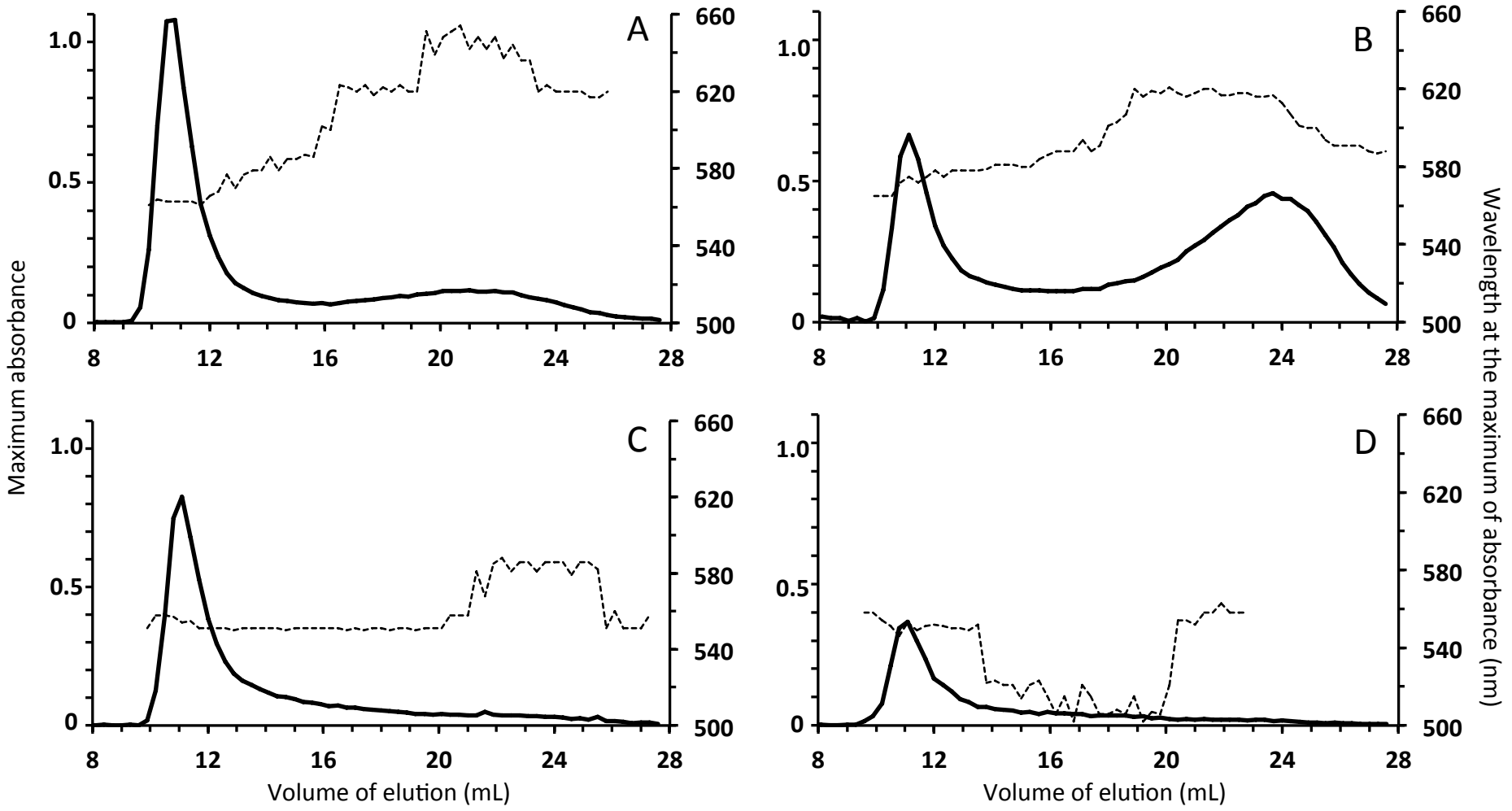


**Figure 8: Fractionation of insoluble polyglucans by size exclusion chromatography.** Purified insoluble polyglucans were dispersed in DMSO, solubilized in NaOH 10 mM and loaded onto a Sepharose® CL-2B matrix. Elution was conducted in NaOH 10 mM at a rate of 12 mL.h$^{-1}$. 300 µL fractions were collected and subsequently analyzed by iodine spectrophotometry. Thick continuous lines are the maximum absorbance of the iodine-polyglucan complexes (left Y-axis). Dashed lines indicate the wavelength (nm) of the iodine-polyglucan complex at the maximum of absorbance (right Y-axis). X-axis is the volume of elution in mL. A: WT; B: β1; C: β12; D: β20.

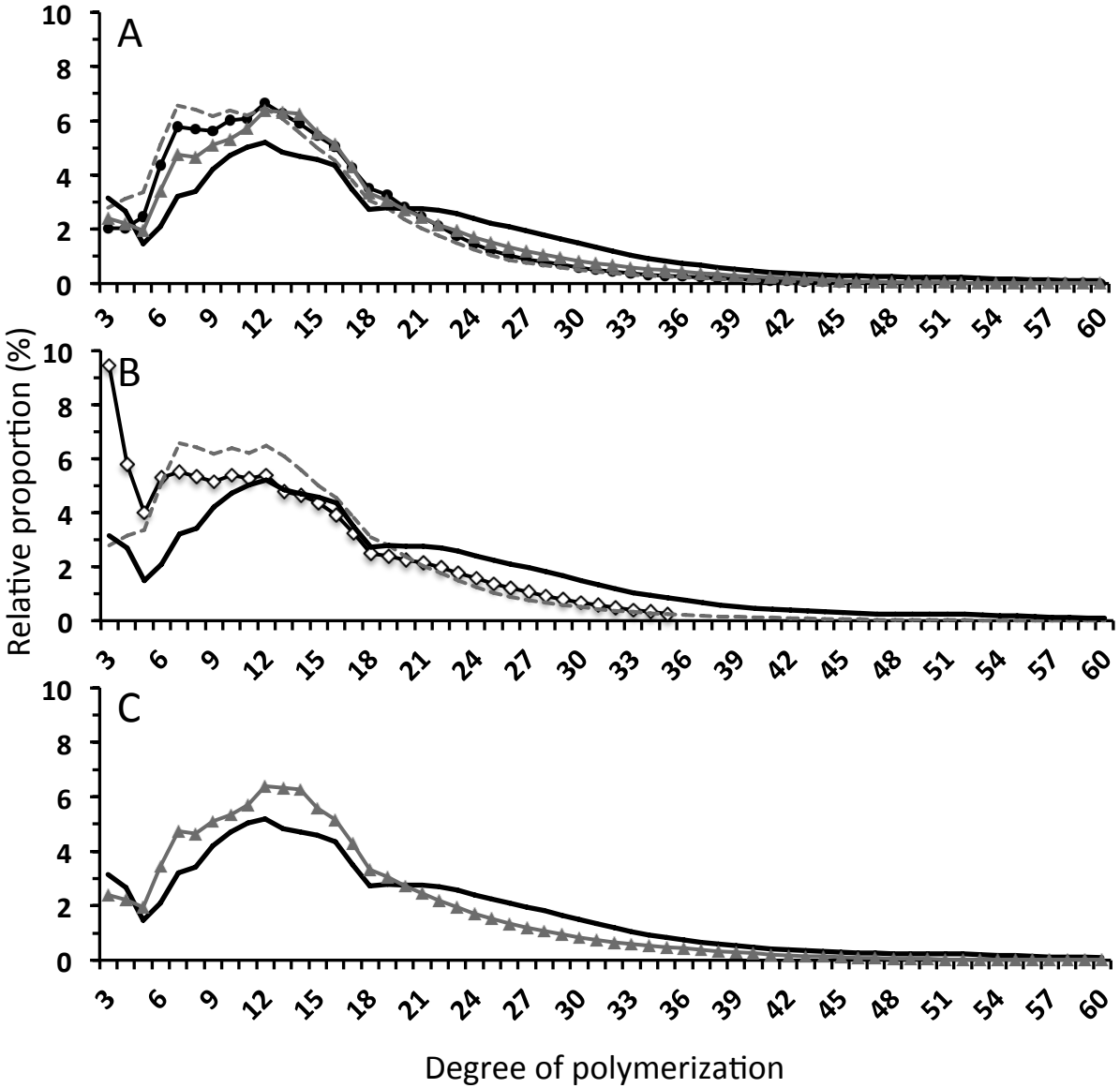


**Figure 9: Chain length distribution of insoluble polyglucans.** Purified insoluble polyglucans were digested with a mix of bacterial debranching enzymes. The corresponding linear glucans were separated by high-performance anion exchange chromatography and detected by pulsed amperometric detection (HPAEC-PAD). The fraction of each DP (from 3 to 60 glucose residues) is expressed in % of the total DP presented on the profile. (A) WT: continuous black line; β1: grey triangles; β12: closed circles; β20: discontinuous grey line. (B) Comparison of the profiles of the WT (continuous black line) and β20 (discontinuous grey line). The profile of the *isa1 isa3 pu1* triple mutant already published in Wattebled et al., 2008 is given (open diamonds). (C) Comparison of the profiles of the WT (continuous black line) and β1 (grey triangles).

**No branching**

⟹ no starch
⟹ no phytoglycogen

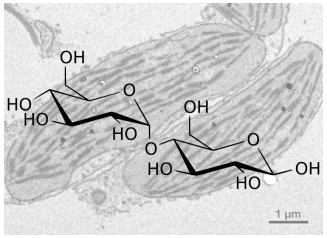


*be2 be3*

**BR/DEBR = 0**

**Balanced or near-balanced branching & debranching**

⟹ starch or starch-like

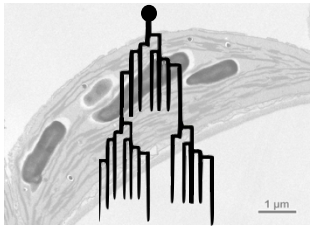


*WT*

**BR/DEBR = optimal**

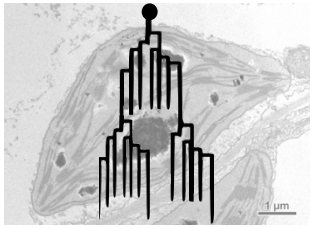


β1

**BR/DEBR ≈ optimal**

**No debranching or high branching**

⟹ no starch
⟹ phytoglycogen or phytoglycogen-like insoluble polyglucan

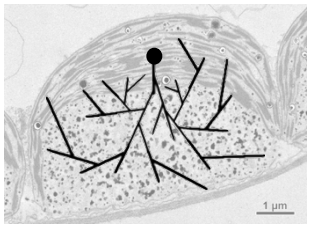


*isa1 isa3 pu1*

**BR/DEBR = ∞**

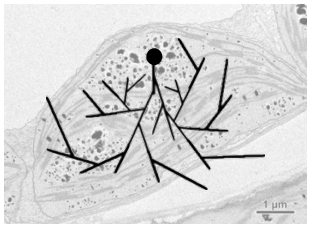


β20

**BR/DEBR >> optimal**

**Figure 10: Starch or starch-like polyglucan synthesis occurs thanks to a balanced branching / debranching activity ratio assuming that starch synthase activity is not limiting whatever the branching/debranching ratio.** Left panel: in the absence of branching activity (*be2 be3* double mutant), starch or phytoglycogen synthesis is impossible and is substituted by maltose accumulation; the BR/DEBR ratio is null. Middle panel: when the ratio BR/DEBR activity is balanced (WT) or near-balanced (β1), starch or starch-like polyglucan synthesis is promoted. In the case of β1, the slight structural modification of starch is due to the expression of the bacterial glycogen-branching enzyme that has different catalytic and regulatory properties. Right panel: in the absence of debranching activity (such as in *isa1 isa3 pu1*; BR/DEBR is infinite) or when branching activity is extremely high (such as in β20; BR/DEBR >> optimal) phytoglycogen or phytoglycogen-like insoluble polyglucan is synthesized respectively. Superimposed drawings correspond to (from left to right): maltose, amylopectin, phytoglycogen; black points depict the reducing end.

**Supplemental Figure S1**

**Description of the approach employed for the synthesis the GlgB chimeric sequence used for expression in *A. thaliana*.**

The chimeric sequence used to transform the *be2 be3* double mutant is composed of the nucleotide sequence of the transit peptide of the plant gene AtBE2 (At5g03650) and the E. coli *glgB* nucleotide sequence (M13751). a) Global scheme of the method is presented. b) Primers nucleotide sequences. Nucleotides in green correspond to the AtBE2 transit peptide sequence and nucleotides in red correspond to the coding sequence of *glgB*. Nucleotides "CACC" highlighted in blue are required for insertion of the sequence in the pENTR/D-TOPO vector. (c) Hybridization temperatures used for each couple of primers and number of cycles used during amplification. (d) Nucleotide and amino acid sequences of the chimeric gene.

## a) Global scheme

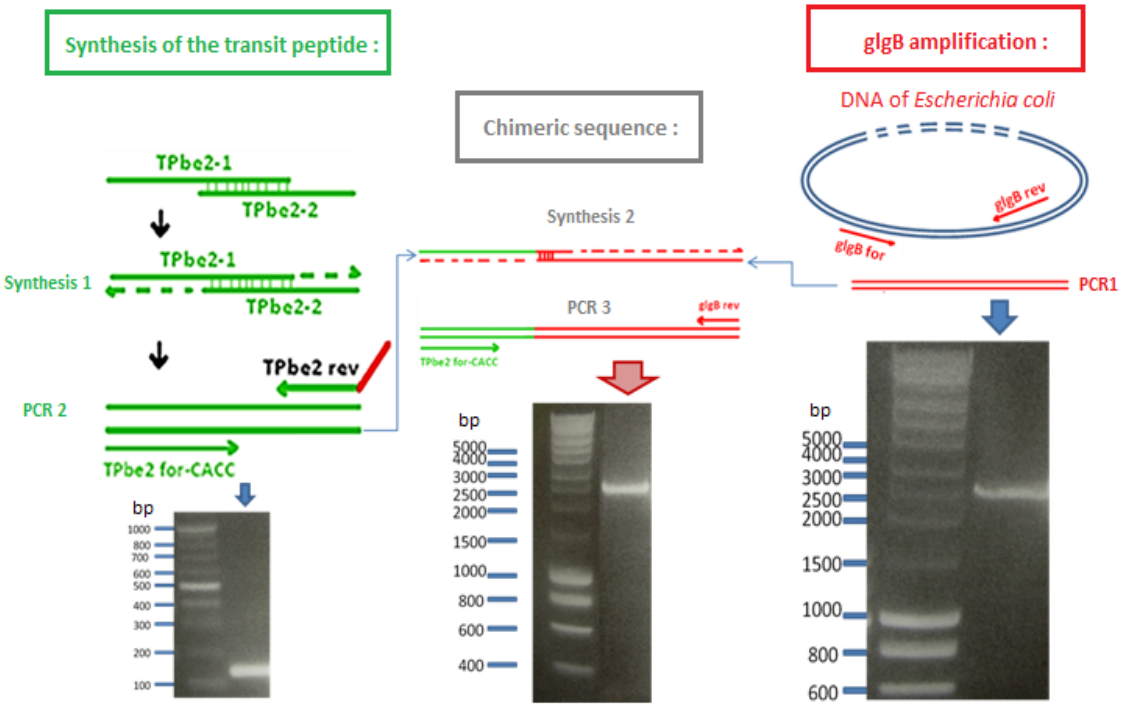


The coding sequence of *glgB* was amplified directly with *E. coli* genomic DNA (PCR1). The transit peptide was synthesized with two long complementary primers (synthesis 1) (PCR2). PCR products 1 and 2 were hybridized to synthesize the chimeric sequence (synthesis 2) and the chimeric sequence was finally amplified (PCR 3) before its insertion in the entry vector.

### b) Primers sequences

| | |
|---|---|
| **glgB for** | atgtccgatcgtatcgatagagacgtgatt |
| **glgB rev** | tcattctgcctcccgaacca |
| **TPbe2-1** | atggtggtgattcacggagtgtctcttactccacgcttcactcttccttctcgacctc tcaacactggctttaatgccggcaattccaccctctctttcttcttcaaaaagcaccc tc |
| **TPbe2-2** | agagatagcttgtgacgaagaatcaaactccgcagattgtttcccagcaaagatcttc cgagagagagggtgctttttgaagaagaaagagagggtgg |
| **TPbe2 for-CACC** | caccatggtggtgattcacggagt |
| **TPbe2 rev** | aatcacgtctctatcgatacgatcggacatagagatagcttgtgacgaagaatca |

### c) PCR conditions

| Primer couples | Hybridization temperatures | Number of cycles |
|---|---|---|
| **PCR1: glgB for / glgB rev** | 61°C | 34 |
| **SYNTHESIS 1: TPbe2-1 / TPbe2-2** | 55°C | 24 |
| **PCR2: TPbe2 for-CACC / Tpbe2 rev** | 54°C | 30 |
| **SYNTHESIS 2: with amplicons from PCR1 & PCR2** | 54°C | 20 |
| **PCR3: TPbe2 for-CACC / glgB rev** | 54°C | 34 |

### d) Chimeric sequences

Nucleotide sequence of the chimeric gene

In green: nucleotides corresponding to the transit peptide of the AtBE2 gene. In red: nucleotides of the coding sequence of *E. coli glgB* gene. In blue, nucleotides required for insertion of the construction into the entry vector. Underlined nucleotides correspond to the primers used for PCR amplification (see table above)

CACCATGGTGGTGATTCACGGAGTGTCTCTTACTCCACGCTTCACTCTTCCTTCTCGACCTCTCAACACTGGCTT
TAATGCCGGCAATTCCACCCTCTCTTTCTTCTTCAAAAAGCACCCTCTCTCTCGGAAGATCTTTGCTGGGAAACA
ATCTGCGGAGTTTGATTCTTCGTCACAAGCTATCTCTATGTCCGATCGTATCGATAGAGACGTGATTAACGCGCT
AATTGCAGGCCATTTTGCGGATCCTTTTTCCGTACTGGGAATGCATAAAACCACCGCGGGACTGGAAGTCCGTGC
CCTTTTACCCGACGCTACCGATGTGTGGGTGATTGAACCGAAAACCGGGCGCAAACTCGCAAAACTGGAGTGTCT
CGACTCACGGGGATTCTTTAGCGGCGTCATTCCGCGACGTAAGAATTTTTTCCGCTATCAGTTGGCTGTTGTCTG
GCATGGTCAGCAAAACCTGATTGATGATCCTTACCGTTTTGGTCCGCTAATCCAGGAAATGGATGCCTGGCTATT
ATCTGAAGGTACTCACCTGCGCCCGTATGAAACCTTAGGCGCGCATGCAGATACTATGGATGGCGTCACAGGTAC
GCGTTTCTCTGTCTGGGCTCCAAACGCCCGTCGGGTCTCGGTGGTTGGGCAATTCAACTACTGGGACGGTCGCCG
TCACCCGATGCGCCTGCGTAAAGAGAGCGGCATCTGGGAACTGTTTATCCCTGGGGCGCATAACGGTCAGCTCTA
TAAATACGAGATGATTGATGCCAATGGCAACTTGCGTCTGAAGTCCGACCCTTATGCCTTTGAAGCGCAAATGCG
CCCGGAAACCGCGTCTCTTATTTGCGGGCTGCCGGAAAAGGTTGTACAGACTGAAGAGCGCAAAAAAGCGAATCA
GTTTGATGCGCCAATCTCTATTTATGAAGTTCACCTGGGTTCCTGGCGTCGCCACACCGACAACAATTTCTGGTT
GAGCTACCGCGAGCTGGCCGATCAACTGGTGCCTTATGCTAAATGGATGGGCTTTACCCACCTCGAACTACTGCC
CATTAACGAGCATCCCTTCGATGGCAGTTGGGGTTATCAGCCAACCGGCCTGTATGCGCCAACCCGCCGTTTTGG
TACTCGCGACGACTTCCGTTATTTCATTGATGCCGCACACGCAGCTGGTCTGAACGTGATTCTCGACTGGGTGCC
AGGCCACTTCCCGACTGATGACTTTGCGCTTGCCGAATTTGATGGCACGAACTTGTATGAACACAGCGATCCGCG

TGAAGGCTATCATCAGGACTGGAACACGCTGATCTACAACTATGGTCGCCGTGAAGTCAGTAACTTCCTCGTCGG
TAACGCGCTTTACTGGATTGAACGTTTTGGTATTGATGCGCTGCGCGTCGATGCGGTGGCGTCAATGATTTATCG
CGACTACAGCCGTAAAGAGGGGGAGTGGATCCCGAACGAATTTGGCGGGCGCGAGAATCTTGAAGCGATTGAATT
CTTGCGTAATACCAACCGTATTCTTGGTGAGCAGGTTTCCGGTGCGGTGACAATGGCTGAGGAGTCTACCGATTT
CCCTGGCGTTTCTCGTCCGCAGGATATGGGCGGTCTGGGCTTCTGGTACAAGTGGAACCTCGGCTGGATGCATGA
CACCCTGGACTACATGAAGCTCGACCCGGTTTATCGTCAGTATCATCACGATAAACTGACCTTCGGGATTCTCTA
CAACTACACTGAAAACTTCGTCCTGCCGTTGTCGCATGATGAAGTGGTCCACGGTAAAAAATCGATTCTCGACCG
CATGCCGGGCGACGCATGGCAGAAATTCGCGAACCTGCGCGCCTACTATGGCTGGATGTGGGCATTCCCGGGCAA
GAAACTACTGTTCATGGGTAACGAATTTGCCCAGGGCCGCGAGTGGAACCATGACGCCAGCCTCGACTGGCATCT
GTTGGAAGGCGGCGATAACTGGCACCACGGTGTCCAGCGTCTGGTGCGCGATCTGAACCTCACCTACCGCCACCA
TAAAGCAATGCATGAACTGGATTTTGACCCGTACGGCTTTGAATGGCTGGTGGTGGATGACAAAGAACGCTCGGT
GCTGATCTTTGTGCGTCGCGATAAAGAGGGTAACGAAATCATCGTTGCCAGTAACTTTACGCCGGTACCGCGTCA
TGATTATCGCTTCGGCATAAACCAGCCGGGCAAATGGCGTGAAATCCTCAATACCGATTCCATGCACTATCACGG
CAGTAATGCAGGCAATGGCGGCACGGTACACAGCGATGAGATTGCCAGCCACGGTCGTCAGCATTCACTAAGCCT
GACGCTACCACCGCTGGCCACTATCTGGCTGGTTCGGGAGGCAGAATGA

Aminoacid sequence of the chimeric GlgB protein (transit peptide in green)

MVVIHGVSLTPRFTLPSRPLNTGFNAGNSTLSFFFKKHPLSRKIFAGKQSAEFDS
SSQAISMSDRIDRDVINALIAGHFADPFSVLGMHKTTAGLEVRALLPDATDVWVI
EPKTGRKLAKLECLDSRGFFSGVIPRRKNFFRYQLAVVWHGQQNLIDDPYRFGPL
IQEMDAWLLSEGTHLRPYETLGAHADTMDGVTGTRFSVWAPNARRVSVVGQFNYW
DGRRHPMRLRKESGIWELFIPGAHNGQLYKYEMIDANGNLRLKSDPYAFEAQMRP
ETASLICGLPEKVVQTEERKKANQFDAPISIYEVHLGSWRRHTDNNFWLSYRELA
DQLVPYAKWMGFTHLELLPINEHPFDGSWGYQPTGLYAPTRRFGTRDDFRYFIDA
AHAAGLNVILDWVPGHFPTDDFALAEFDGTNLYEHSDPREGYHQDWNTLIYNYGR
REVSNFLVGNALYWIERFGIDALRVDAVASMIYRDYSRKEGEWIPNEFGGRENLE
AIEFLRNTNRILGEQVSGAVTMAEESTDFPGVSRPQDMGGLGFWYKWNLGWMHDT
LDYMKLDPVYRQYHHDKLTFGILYNYTENFVLPLSHDEVVHGKKSILDRMPGDAW
QKFANLRAYYGWMWAFPGKKLLFMGNEFAQGREWNHDASLDWHLLEGGDNWHHGV
QRLVRDLNLTYRHHKAMHELDFDPYGFEWLVVDDKERSVLIFVRRDKEGNEIIVA
SNFTPVPRHDYRFGINQPGKWREILNTDSMHYHGSNAGNGGTVHSDEIASHGRQH
SLSLTLPPLATIWLVREAE

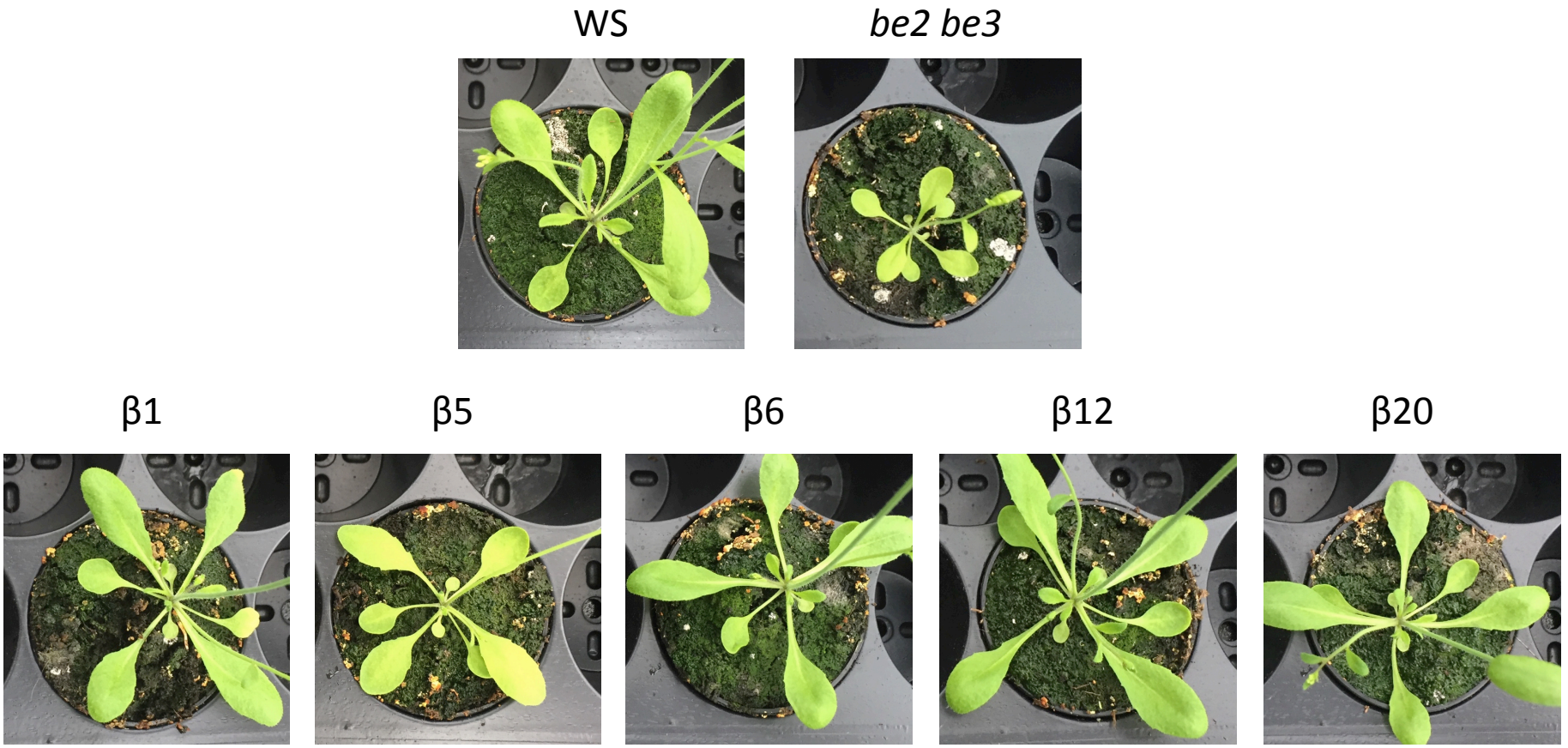


**Supplemental Figure S2: comparison of mature plant size.** Seeds were sown on peat-based compost and plants were grown in greenhouse for 16h in the light at 21°C and 8h in the dark and 16°C. Pictures were taken 3 weeks after germination. The *be2 be3* double mutant has a strong growth retardation phenotype and plants are much smaller than wild type (Dumez et al., 2006) whereas all transformed plants expressing *E. coli* GlgB branching enzyme have a phenotype close to that of the wild type reference.

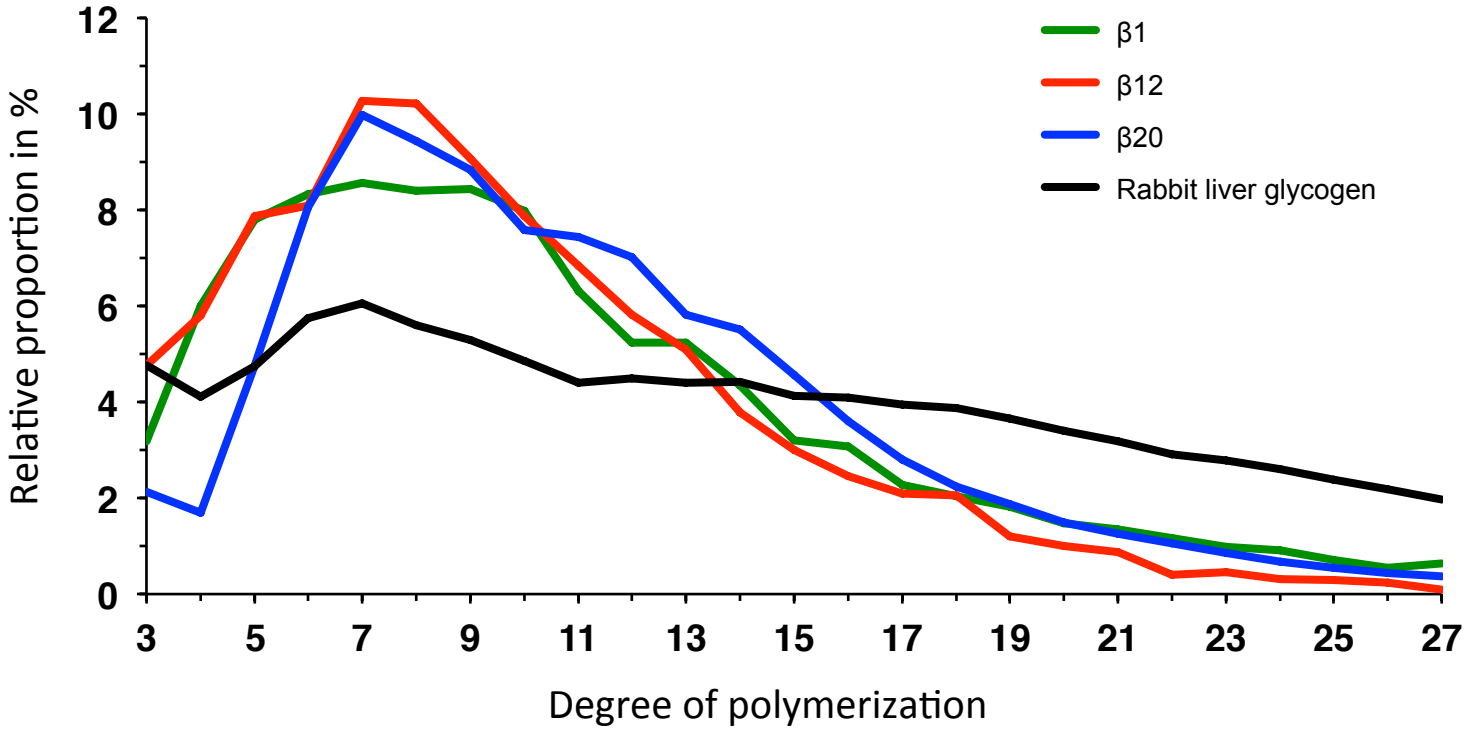


**Supplemental Figure S3: Chain length distribution profiles of water soluble polyglucans** purified from GlgB-expressing lines β1 (green), β12 (red) and β20 (blue) compared to that of the rabbit liver glycogen (black). After purification, water soluble polyglucans were debranched by a mix of bacterial isoamylase and pullulanase. The branched products were analyzed by HPAEC-PAD. The relative proportion of each glucan is plotted versus their degree of polymerization. Values are the mean of two analysis carried out with soluble polyglucans extracted of plants cultivated independently.

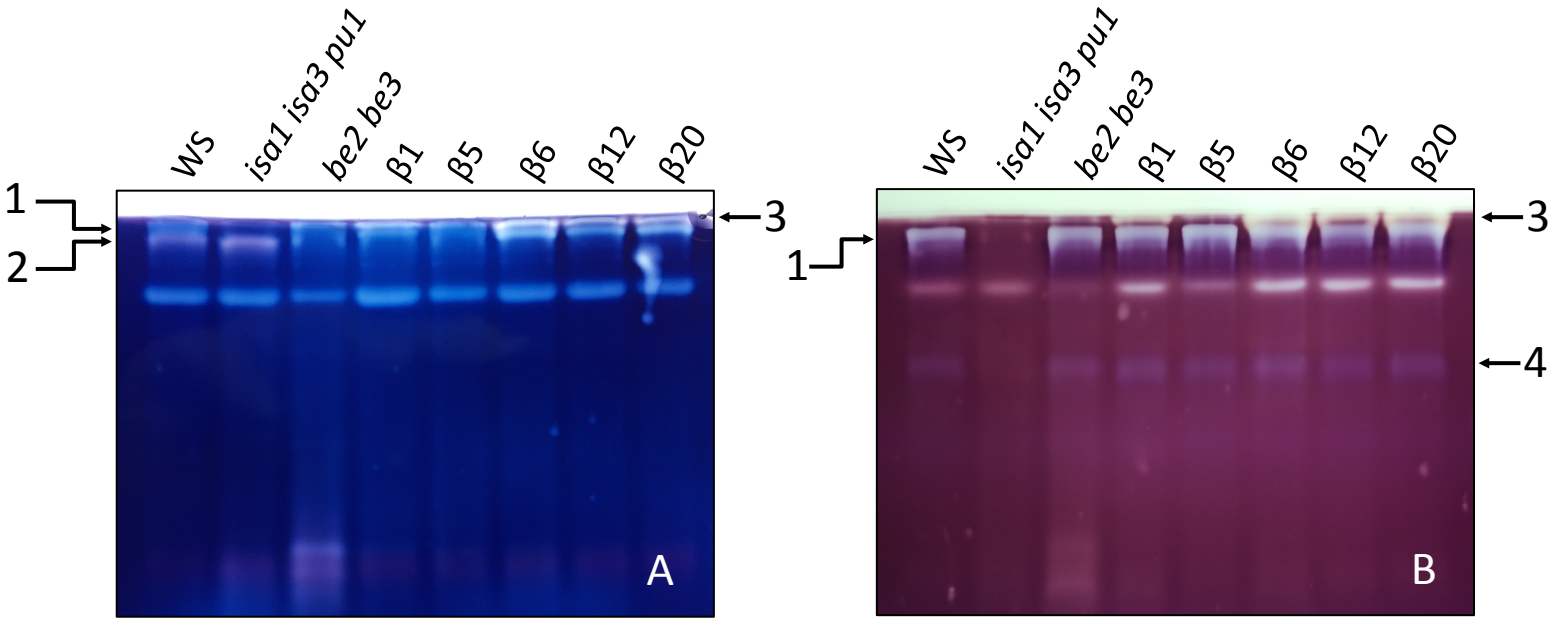


**Supplemental Figure S4: Zymogram analysis of transformed plant expressing GlgB.** Three to four leaves of 3 week-old plants were harvested at mid-day for soluble extract preparation. The equivalent of 50 µg of proteins were loaded on polyacrylamide gel impregnated with either 0.3% of potato soluble starch (A) or 0.3% of maize β-limit dextrins (B). After migration (2 h at 4°C, 15 mA / gel), the gels were incubated overnight at room temperature in a buffer composed of : Tris 25 mM; Glycine 192 mM; $MgCl_2$ 1 mM; $CaCl_2$ 1 mM; DTT 10 mM. After incubation, enzymes that modified the substrate were revealed by soaking the gels in iodine solution (1% KI [w/v]; 0.1% $I_2$ [w/v]). The gels were rinsed in water before taking pictures. WS is the wild type reference (*Wassilewskija*) and all other plants are in the same genetic background. *be2 be3* corresponds to a double mutant lacking endogenous branching enzymes. β1, β5, β6, β12, and β20 are *be2 be3* mutants expressing different levels of *E. coli* GlgB. Blue Band labeled 1 and red band labeled 2 were previously determined as Iso1 and BE2 respectively (Dumez et al., 2006; Wattebled et al., 2008). The pale pink band labeled 3 with an extremely low mobility, present only in transformed plants, corresponds to GlgB. Band 4 is the pullulanase (Wattebled et al., 2008).

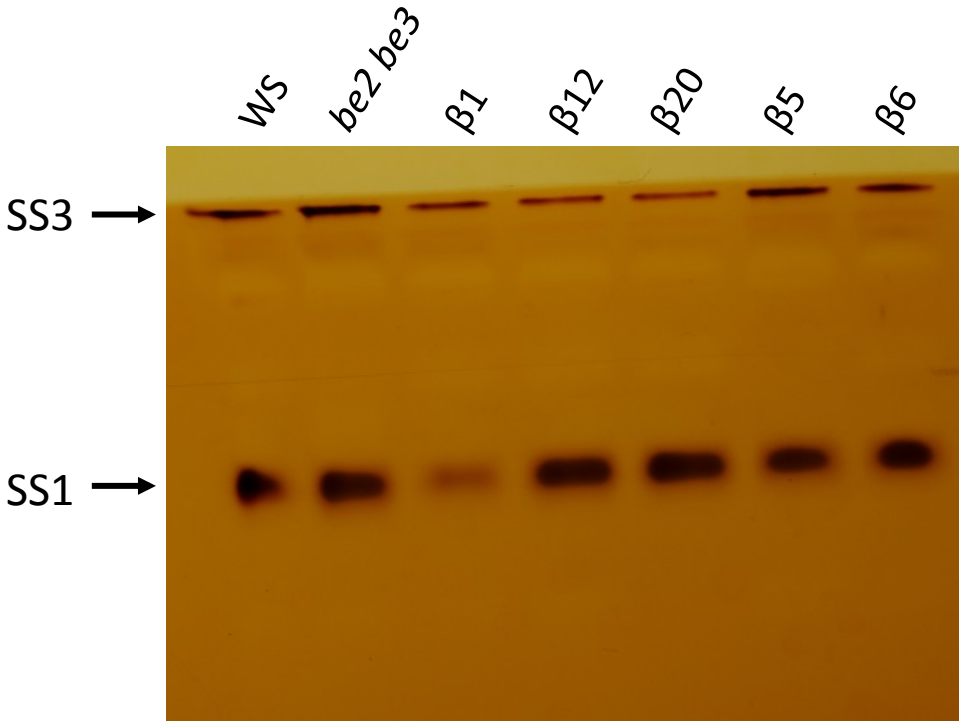


**Supplemental Figure S5: Zymogram analysis of soluble starch synthases activities.** An equal amount of proteins from leaf crude extracts was loaded on native PAGE containing 0.3% (w/v) of rabbit liver glycogen. Approximately 2h30 of migration in native conditions (Tris-glycine buffer 1X, 4°C) was applied. After incubation in an appropriate buffer for starch synthase activity (Glycyl-glycine 66 mM (pH 7.5); $(NH_4)_2SO_4$ 66 mM; $MgCl_2$ 1 mM; β-mercaptoethanol 3.3 mM; ADP-glucose 1.2 mM), the gel was washed 6 times into water to remove β-mercaptoethanol and further incubated in iodine solution until revelation of bands of activity. This zymogram is representative of three biological independent experiments.

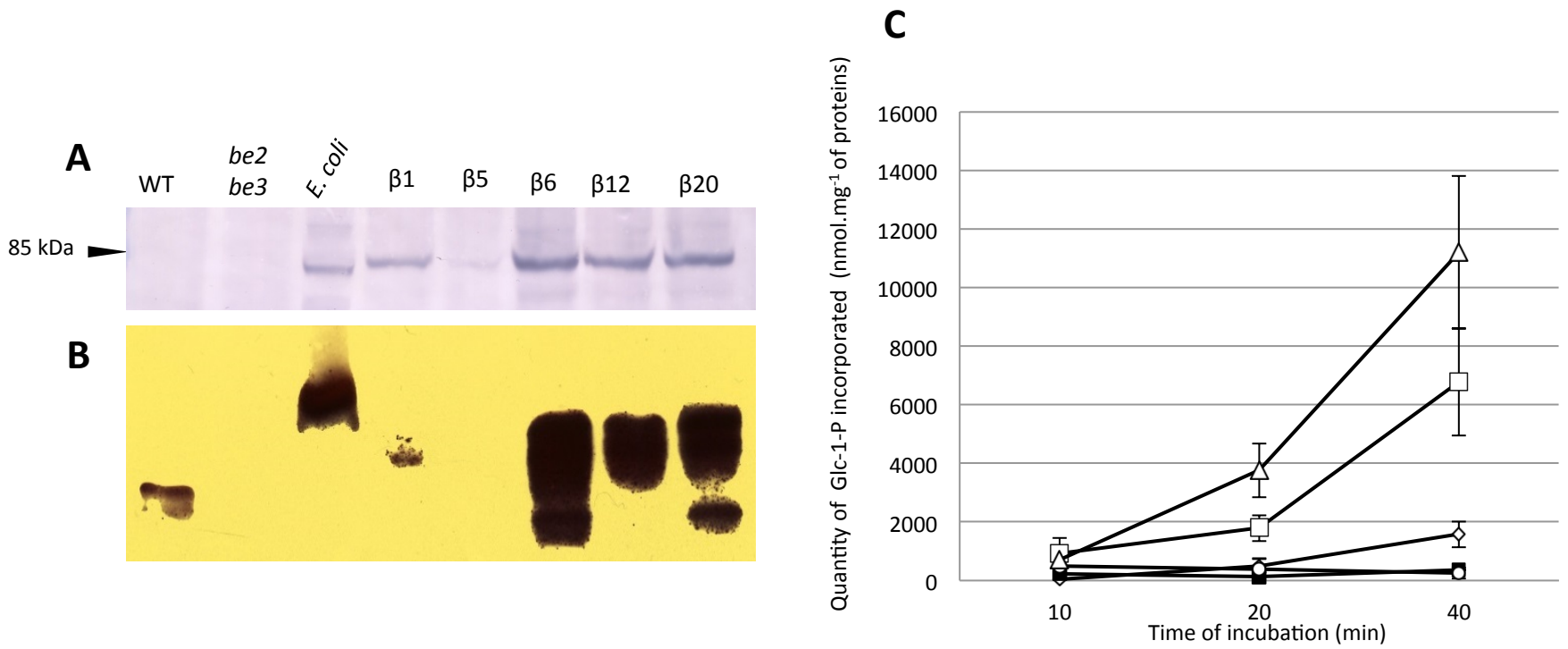


**Supplemental Figure S6 : Expression of glgB in the *be2 be3* transformed lines.** (A) Immunoblot analysis performed in denaturing conditions. Protein extracts were denatured before and during migration in the polyacrylamide gel. After migration, proteins were blotted onto a nitrocellulose membrane and hybridized with a peptide-directed antibody raised against GlgB. (B) zymogram of branching enzyme activity. The polyacrylamide gel contains DP7 maltooligosaccharides and phosphorylase "a". Branching enzyme activity was revealed by incubating the gel for 2 hours in a phosphorylase "a" stimulating buffer. Bands of branched polyglucans were detected by soaking the gel in iodine solution. (C) *in vitro* assay of branching enzyme activity. Protein extracts were incubated for 10 to 40 min in a buffer containing DP7 maltooligosaccharides, phosphorylase "a" and [U-$^{14}$C]Glc-1-P (7.4 kBq per assay) at 50 mM final concentration. The mean of incorporated Glc into branched polyglucans was calculated for 3 independent assays and plotted against the time of incubation. Vertcical lines stand for standard deviation. Open diamonds: WT extract; closed squares: *be2 be3* mutant; open squares: β12; open circles: β5; open triangles: β6.

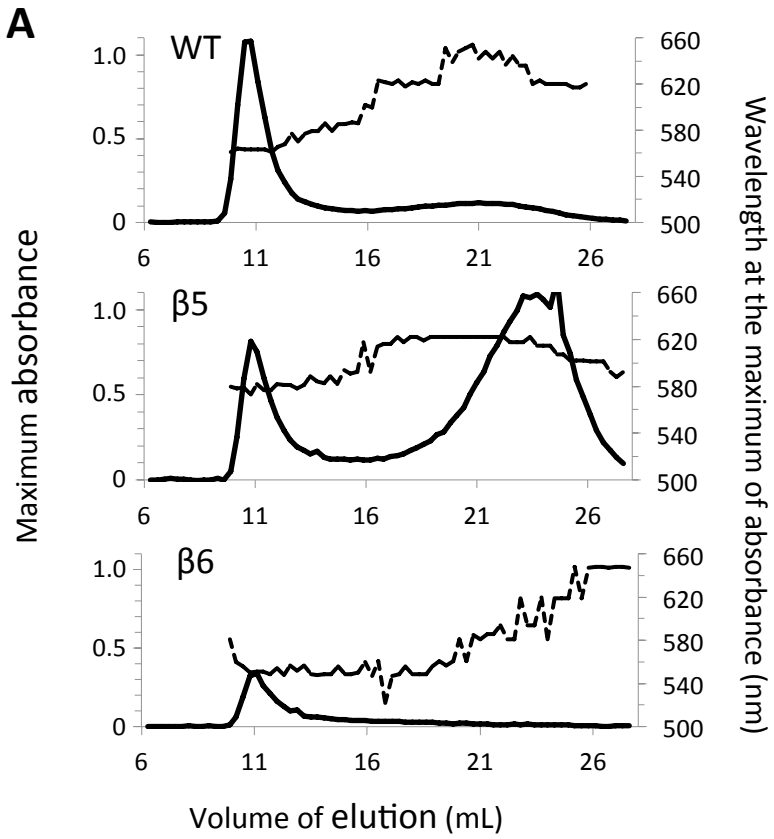


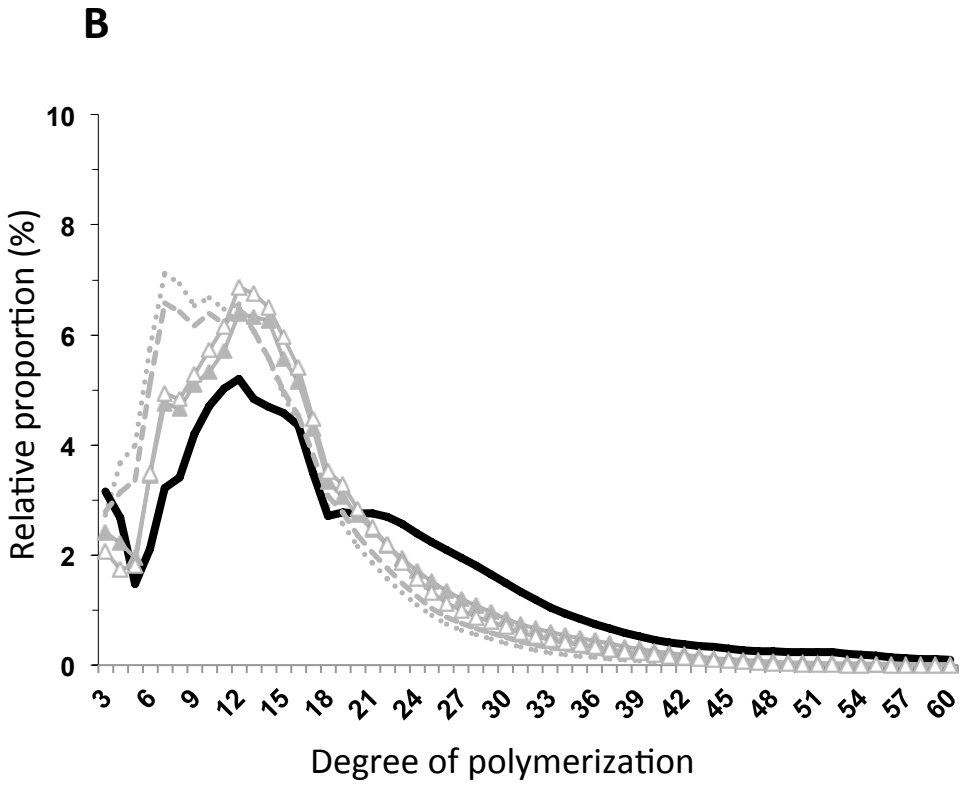


C

| Sample | WT | β5 | β12 | β6 |
|---|---|---|---|---|
| Branching degree (%) | 5.1 | 6.2 | 6.8 | 7.8 |
| $\lambda_{max}$ of amylopectin (nm) | 563 | 571 | 553 | 545 |
| Crystallinity index (%) | 33 | 23 | 20 | 15 |

**Supplemental Figure S7 : Structure of polysaccharides produced in β5 and β6 transformant lines.**

**(A) Fractionation of insoluble polyglucans by size exclusion chromatography.** Dashed lines indicate the wavelength (nm) of the iodine-polyglucan complex at the maximum of absorbance (right Y-axis).

**(B) Chain length distribution of insoluble polyglucans.** WT: continuous black line; β1: closed grey triangles; β5: open grey triangles ; β6: dotted grey line; β20: discontinuous grey line.

**(C) Structural parameters of polysaccharides produced in β5 and β6 tranformant lines**. The branching degree was calculated according to Szydlowski et al. (2011).

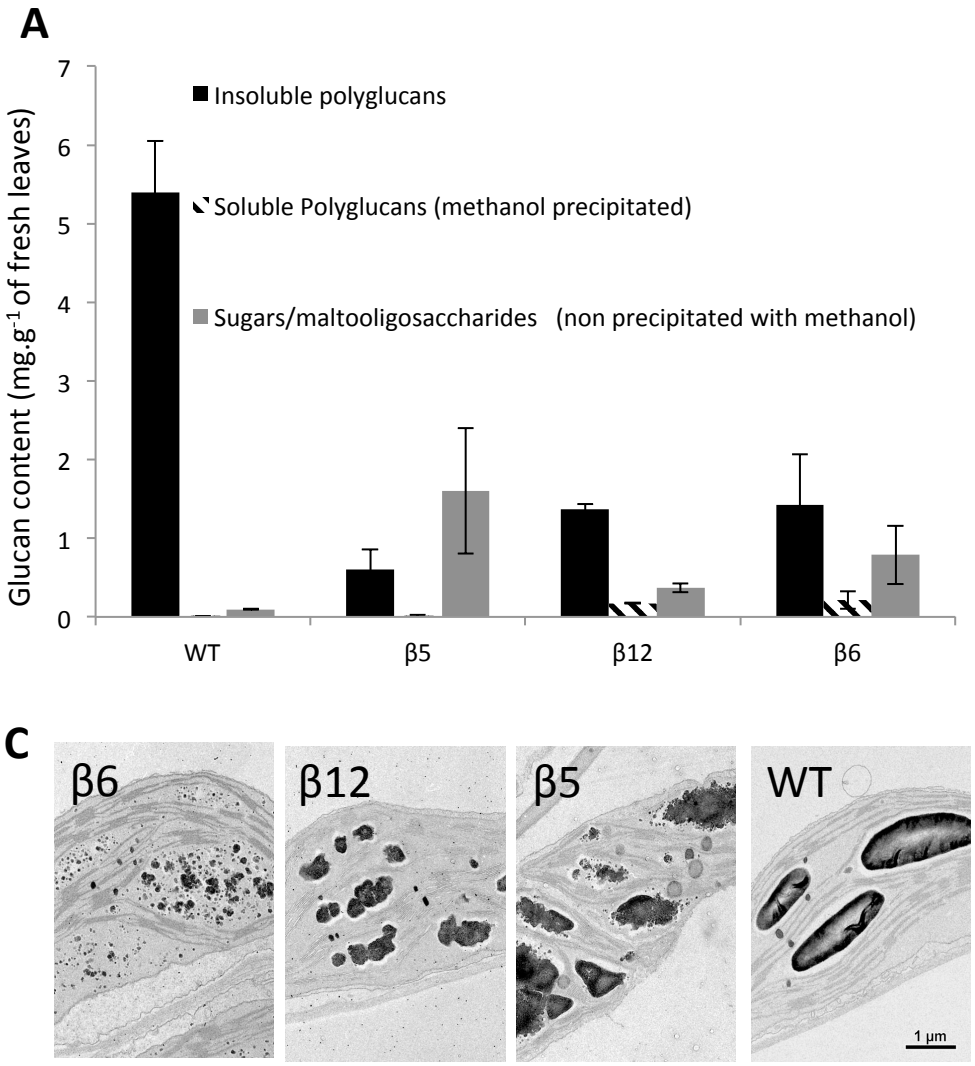


**Supplemental Figure S8 : Leaf glucan contents and granules morphology.**

A: For glucan content the average of three independent cultures are presented. Vertical thin bars are the standard deviation of three independent biological replicates. B: Scanning electron microscopy images of purified insoluble polyglucans. C: Transmission electron microscocopy images of leaf chloroplasts positively stained with PATAg.